Mapping central circuits for leg somatosensation in *Drosophila*

Su-Yee Lee

A dissertation

submitted in partial fulfillment of the

requirements for the degree of

Doctor of Philosophy

University of Washington

2024

Reading Committee:

John C. Tuthill, Chair

Jan-Marino Ramirez

Amy Orsborn

Program Authorized to Offer Degree:

Neuroscience

University of Washington

Abstract

Mapping central circuits for leg somatosensation in *Drosophila*

Su-Yee Lee

Chair of the Supervisory Committee:
John C. Tuthill
Physiology and Biophysics

Animal movement relies on precise and adaptive sensing of the body, known as somatosensation. Although somatosensory feedback is essential for optimal movement, its underlying mechanisms remain unclear. A major challenge in studying somatosensory systems, especially when working with diverse animal models, is understanding the specific roles and contexts in which this sensory information is utilized. In this thesis, we investigate the connectivity and modulation of the femoral chordotonal organ (FeCO), the largest somatosensory structure in the fly leg, to discern its function. While the FeCO is established as a proprioceptive organ that senses position and movement of the leg, our understanding of its functions remain limited. In Chapter 2, we present the most comprehensive synaptic wiring diagram of the FeCO to date, mapping its downstream circuitry within the ventral nerve cord and brain. Notably, we identified new pathways connecting the FeCO to auditory circuits in the brain, supporting the emerging hypothesis that the FeCO detects externally generated substrate vibrations. In Chapter 3, we present unpublished work investigating state-dependent modulation of the FeCO, focusing on how neuropeptides contextually tune transmission of vibration sensing to alter sensory perceptions. In contrast to the

synaptic wiring diagram, this work provides an experimental framework for investigating extrasynaptic modulation of FeCO sensory activity and related behaviors. Finally, in Chapter 4, we conclude with future directions to experimentally test the predictions derived from this research.

TABLE OF CONTENTS

LIST OF FIGURES

LIST OF TABLES

ACKNOWLEDGEMENTS

I am surrounded by many wonderful colleagues, friends, and family members who helped make my Ph.D. possible. I have countless people to thank, but here is the shortlist.

First, I want to thank my advisor, John Tuthill, for unwavering support and dedicated mentorship. Since our first meeting, you have consistently inspired and encouraged me to lean into curiosity without justification and face challenges without fear. Thank you for investing so much time and attention towards my training. I am proud and honored to be one of your first Ph.D. students. Second, I want to acknowledge my close collaborators: Sweta Agrawal and Chris Dallmann, for sharing your projects and experimental rigs with me. Thank you for your generosity, patience, and wisdom - working together has been fulfilling and energizing. Thank you to my thesis committee: Nino Ramirez, Tom Daniel, and Amy Orsborn, for guiding me through every milestone with both critical feedback and gracious encouragement. Every year, I left my committee meetings with a renewed sense of joy for the work. Additional thanks to other advisors who helped me make the leap to graduate school: Ethan McBride, Ed Callaway, John Scott, and Sonal Thakar, for creating the spaces where my love for neuroscience grew.

To the Tuthill lab, a vibrant community of scientists who care deeply about their work and each other: this thesis stands on the foundation of our collective work. You all inspired and supported me every day, both scientifically and personally. During the pandemic especially, you were some of the only people I saw and really trusted – for that I am grateful. Thank you to Akira Mamiya, for showing me how to dissect and record from tiny nervous systems, the skill I am most proud of. Thank you to Anne Sustar, for your expertise and diligence in maintaining the fly stocks, which I often turned to for convenience (and sometimes salvation). Thank you to my Ph.D. cohort:

Ellen, Brandon, and Lili, for the friendship and fellowship; To close colleagues who became friends: Todd, Adree, and Raveena, for the daily debriefs and rotations of allergen-free snacks.

Thanks to my friends and family who made my life so much brighter: Reggie, for the hugs, adventures, and picking up every time I call; Mabel, for reminding me to take breaks; Tess and Sara, for being my sisters; Jordan, for solidarity; my family, near and far, for moving mountains for my education; my nephews and nieces (Joseph, Noah, Charbel Jr., Olivia, Madeleine, and Sophia) for making me laugh and keeping me humble. Eternal thanks to my mom, Evelyn, who filled our life with books and taught me to be curious and critical of the world.

DEDICATION

To my friends and family

Chapter 1

INTRODUCTION

Background

Somatosensation

Somatosensation, the sense of the body, is constructed from the activity of distributed sensors that detect mechanical movement, temperature, and chemicals[1]. In this thesis, we focus on mechanosensory neurons that respond to mechanical stretch, tension, and load. In contrast to other sensory neurons that are housed in compact, specialized sensory systems (e.g. retina in the eye or cochlea of the ear), somatosensory neurons are broadly distributed in varied and highly mobile body parts and tissues (e.g. muscles and tendons)[2,3]. As a result of their embedding in the musculoskeletal system, mechanosensory neurons can detect both internally- and externally-generated mechanical forces. For example, rodents have vibration-sensitive Pacinian Corpuscles that detect both externally-generated vibrations and skeletal vibrations produced through self-generated movements[4]. Understanding the location, origin, and significance of the mechanical stimuli acting on an animal's body is critical for adaptive motor behavior. If the forces are an expected consequence of self-movement, then the animal should ignore the stimulus. If the forces are due to salient, external perturbations, then the animal should respond appropriately.

Delineating the type of information that mechanosensory neurons are tuned to and how this information is transmitted to inform motor behavior is a non-trivial challenge for experimentalists. Recordings are often performed in reduced preparations where animal movement is restricted and

passive stimuli are applied. Measuring patterns of force distribution within the bodies of behaving animals is often not feasible. It is also challenging to record from somatosensory neurons and quantify their encoding properties under naturalistic conditions. Thus, much of our understanding of the response properties, or receptive fields, of somatosensory neurons come from measurements in immobilized animals in response to calibrated mechanical stimuli. Under these constrained experimental conditions, it is difficult to probe the full, naturalistic range of stimuli and further, distinguish what information, whether self- or externally-generated, is saliently transmitted to central circuits to inform motor control.

Chordotonal Organs: A Model System for Studying Somatosensation

Chordotonal organs, stretch receptors uniquely found in insects and crustaceans, are historically used as model systems for studying somatosensory feedback onto motor circuits and the sense of hearing[5,6]. Chordotonal organs have a unique evolutionary history that point to the close relationship between proprioceptors and exteroceptors. In insects, some initially proprioceptive chordotonal organs evolved a sensitivity to externally generated airborne vibrations – developing the sense of hearing[7]. While much is known about the structural adaptations in chordotonal organs that support the sense of hearing, less is known about the neural circuitry adapted to parse self-generated vs externally-generated information[8]. Are chordotonal organs structurally adapted to receive only proprioceptive or exteroceptive information, or do they receive a mix of both? If the information is mixed, what are the neural mechanisms used to dissociate the salient, multi-modal signals?

Across insects and crustaceans, chordotonal organs have reportedly mixed proprioceptive and exteroceptive capabilities, but investigations on these structures are usually focused on one

type or the other. The antennal Johnston's organ, for example, is primarily studied for its sensitivity to auditory stimuli, although it can also sense position and movement of the antennae[9–11]. In contrast, the femoral chordotonal organ (FeCO), located in the femur-tibia joint of the insect leg, is largely considered a proprioceptive structure that detects self-generated movement and position of the legs. Across insects, the FeCO has been used as a model organism for proprioceptive feedback for motor behaviors such as reflex reversal, postural control, and locomotion[10,11].

Recent work in the *Drosophila* FeCO provides insight into the anatomical and circuit mechanisms supporting its dual proprioceptive and exteroceptive functions. The FeCO has three functionally and anatomically distinct sensory subtypes: claw neurons sense tibia position, hook neurons sense tibia movement, and club neurons sense tibia movement and vibration[14,15]. Although the FeCO is responsive to vibration, it is unclear if these vibration-sensing capacities are functionally relevant or a byproduct of its proprioceptive sensing. A few studies suggest that fruit flies rely on the FeCO to detect substrate vibrations for predator detection and social communication[16–18]. Otherwise, there is very little known about the ethological relevance and neural mechanisms for substrate vibration sensing. As a step towards understanding the central processing of FeCO information, Agrawal et al.[19] and Chen et al.[20] recorded from second-order FeCO neurons, revealing complex mixing of position, movement, and vibration information. Overall, while the experimental work in *Drosophila* FeCO reveals that it is capable of detecting both proprioceptive and exteroceptive information, it is still unclear how the central nervous system processes this mixed information.

Thesis Overview

In this thesis, we developed new methods for investigating how proprioceptive and exteroceptive information detected by the FeCO is centrally processed in the nervous system to inform behavior. This work started with a broad screen through neuromodulatory systems in *Drosophila* and their effects on sensorimotor circuits and behavior, described in Chapter 3. Sensory neurons are not just rote stimuli detectors and are subject to context-dependent modulation that alters the transmission of sensory information. Looking at the modulation of sensory encoding gives insight into extrasynaptic mechanisms that transform sensory detection into sensory perception in accordance with the state of the organism. Through this screen, we focused specifically on how two neuropeptides, Allatostatin A and Myosuppressin, modulate vibration sensing. At the time, it was unclear how *Drosophila* use vibration information sensed by the legs, if at all. By studying the modulation of the mysterious leg vibration sense, this motivated us to use alternative methods to elucidate the ethological relevance of vibration sensing in the FeCO. To this end, we constructed the FeCO connectome, a synaptic wiring diagram that spans the ventral nerve cord and the brain, presented in Chapter 2. We mapped the downstream circuitry from the FeCO sensory neurons to motor and sensory circuits to infer how the FeCO informs different motor behaviors such as postural control, walking, and escape. Notably, we found that the FeCO vibration sensors connect to divergent pathways from the proprioceptors, ultimately integrating with exteroceptive auditory circuits in the brain. Overall, this work generates data-driven hypotheses about the function of an insect somatosensory structure. In the final chapter, I outline some concrete future directions to expand and test these hypotheses.

References

1. The Somatosensory System: Receptors and Central Pathways. in *Principles of Neural Science, Fifth Edition* (McGraw-Hill Education, New York, NY, 2014).
2. Tuthill, J. C. & Wilson, R. I. Mechanosensation and Adaptive Motor Control in Insects. *Curr. Biol.* **26**, R1022–R1038 (2016).
3. Tuthill, J. C. & Azim, E. Proprioception. *Curr. Biol.* **28**, R194–R203 (2018).
4. Turecek, J. & Ginty, D. D. Coding of self and environment by Pacinian neurons in freely moving animals. *BioRxiv Prepr. Serv. Biol.* 2023.09.11.557225 (2023) doi:10.1101/2023.09.11.557225.
5. Field, L. & Matheson, T. Chordotonal Organs of Insects. *Adv. Insect Physiol. - ADVAN INSECT PHYSIOL* **27**, (1998).
6. Cohen, M. J. The crustacean myochordotonal organ as a proprioceptive system. *Comp. Biochem. Physiol.* **8**, 223–243 (1963).
7. Yack, J. E. & Fullard, J. H. What is an Insect Ear? *Ann. Entomol. Soc. Am.* **86**, 677–682 (1993).
8. Yack, J. E. The structure and function of auditory chordotonal organs in insects. *Microsc. Res. Tech.* **63**, 315–337 (2004).
9. Göpfert, M. C. & Robert, D. The mechanical basis of Drosophila audition. *J. Exp. Biol.* **205**, 1199–1208 (2002).
10. Kamikouchi, A., Shimada, T. & Ito, K. Comprehensive classification of the auditory sensory projections in the brain of the fruit fly Drosophila melanogaster. *J. Comp. Neurol.* **499**, 317–356 (2006).

11. Yorozu, S. *et al.* Distinct sensory representations of wind and near-field sound in the Drosophila brain. *Nature* **458**, 201–205 (2009).

12. Zill, S. N. Selective mechanical stimulation of an identified proprioceptor in freely moving locusts: role of resistance reflexes in active posture. *Brain Res.* **417**, 195–198 (1987).

13. Mendes, C. S., Bartos, I., Akay, T., Márka, S. & Mann, R. S. Quantification of gait parameters in freely walking wild type and sensory deprived Drosophila melanogaster. *eLife* **2**, e00231 (2013).

14. Mamiya, A., Gurung, P. & Tuthill, J. C. Neural Coding of Leg Proprioception in Drosophila. *Neuron* **100**, 636-650.e6 (2018).

15. Mamiya, A. *et al.* Biomechanical origins of proprioceptor feature selectivity and topographic maps in the *Drosophila* leg. *Neuron* **111**, 3230-3243.e14 (2023).

16. Eberhard, M. J. B. *et al.* Structure and sensory physiology of the leg scolopidial organs in Mantophasmatodea and their role in vibrational communication. *Arthropod Struct. Dev.* **39**, 230–241 (2010).

17. Takanashi, T., Fukaya, M., Nakamuta, K., Skals, N. & Nishino, H. Substrate vibrations mediate behavioral responses via femoral chordotonal organs in a cerambycid beetle. *Zool. Lett.* **2**, 18 (2016).

18. McKelvey, E. G. Z. *et al.* Drosophila females receive male substrate-borne signals through specific leg neurons during courtship. *Curr. Biol.* **31**, 3894-3904.e5 (2021).

19. Agrawal, S. *et al.* Central processing of leg proprioception in *Drosophila*. *eLife* **9**, e60299 (2020).

20. Chen, C. *et al.* Functional architecture of neural circuits for leg proprioception in *Drosophila*. *Curr. Biol.* **31**, 5163-5175.e7 (2021).

Chapter 2

DIVERGENT NEURAL CIRCUITS FOR PROPRIOCEPTIVE AND EXTEROCEPTIVE SENSING OF THE *DROSOPHILA* LEG

Authors: Su-Yee J. Lee, Chris J. Dallmann, Andrew Cook, John C. Tuthill*, Sweta Agrawal*

*Equal Contribution

2.0.1 Note

A version of this Chapter was submitted for review and posted as a preprint on *BioRxiv* in 2024[1].

2.1 Abstract

Somatosensory neurons provide the nervous system with information about mechanical forces originating inside and outside the body. Here, we use connectomics to reconstruct and analyze neural circuits downstream of the largest somatosensory organ in the *Drosophila* leg, the femoral chordotonal organ (FeCO). The FeCO has been proposed to support both proprioceptive sensing of the fly's femur-tibia joint and exteroceptive sensing of substrate vibrations, but it remains unknown which sensory neurons and central circuits contribute to each of these functions. We found that different subtypes of FeCO sensory neurons feed into distinct proprioceptive and exteroceptive pathways. Position- and movement-encoding FeCO neurons connect to local leg

motor control circuits in the ventral nerve cord (VNC), indicating a proprioceptive function. In contrast, signals from the vibration-encoding FeCO neurons are integrated across legs and transmitted to auditory regions in the brain, indicating an exteroceptive function. Overall, our analyses reveal the structure of specialized circuits for processing proprioceptive and exteroceptive signals from the fly leg. They also demonstrate how analyzing patterns of synaptic connectivity can distill organizing principles from complex sensorimotor circuits.

2.2 Introduction

To coordinate complex behaviors, circuits in the central nervous system (CNS) require continuous information about the body and the environment. An important source of feedback are somatosensory neurons, which provide the nervous system with information about mechanical forces acting on an animal's body[2,3]. Somatosensory neurons are typically described as either exteroceptive, detecting mechanical forces generated in the external world, or proprioceptive, detecting the position or movement of body parts. However, because they are embedded within the body, many somatosensory neurons can detect both externally- and self-generated forces, making it difficult to determine whether specific somatosensory neurons are exteroceptive, proprioceptive, or both. Recording from primary somatosensory neurons in behaving animals can resolve the types of mechanical stimuli they encode[4], but such experiments are technically difficult and often not feasible. An alternative approach is to map the connectivity of sensory neurons with downstream circuits, which can provide clues to about putative function. For example, some proprioceptor axons synapse directly onto motor neurons to generate rapid reflexes[5] (**Figure 1A**). Somatosensory signals can also be integrated with other sensory cues and internal states to inform action selection in response to external perturbations[6,7].

Mapping the flow of sensory signals into the nervous system has recently become feasible in small organisms thanks to advances in serial-section electron microscopy (EM) and computational image segmentation, which enable the reconstruction of whole synaptic wiring diagrams, or connectomes. Some of the most comprehensive connectomes reconstructed to date include the brain and ventral nerve cord (VNC) of the adult fruit fly, *Drosophila melanogaster*[8–12]. The fly brain connectomes have already revealed new insight into the organization and function of sensory organs on the head. For example, mapping the projections of mechanosensory neurons from the fly's antenna into the brain revealed the organization of circuits that support song detection, antennal grooming, and escape[13,14]. Volumetric EM datasets of the fly VNC[9,10], which is analogous to the vertebrate spinal cord, now make it possible to reconstruct and analyze the function of somatosensory signals from other parts of the fly's body, including the legs and wings.

In this study, we use connectomic analyses of brain and VNC circuits to investigate the largest somatosensory organ in the *Drosophila* leg, the femoral chordotonal organ (FeCO) (**Figure 2.1B**). The *Drosophila* FeCO is comprised of ~150 excitatory (cholinergic) sensory neurons that can be separated into five functionally and anatomically distinct subtypes: (1) extension- and (2) flexion-encoding claw neurons encode tibia position, (3) extension- and (4) flexion-encoding hook neurons sense tibia movement, and (5) club neurons encode bidirectional tibia movement and low-amplitude (<1 μm), high frequency vibration (**Figure 2.1C-D**)[15,16]. The cell bodies and dendrites of the FeCO are located in the femur of each leg and their axons project into the VNC (**Figure 2.1B**)[15–18].

The FeCO is typically described as a proprioceptive organ that monitors the movement and position of the femur-tibia joint[16,19,20]. However, behavioral evidence suggests that the FeCO may also detect externally-generated substrate vibrations, perhaps to aid in social communication,

predator detection, and courtship[21–24]. It is currently unknown to what degree the five subtypes of FeCO sensory neurons are specialized to support specific proprioceptive or exteroceptive functions. The club neurons are the only FeCO subtype that respond to tibia vibration (**Figure 2.1D**), suggesting that they may support exteroceptive vibration sensing[15,16]. However, club neurons also respond to larger movements of the tibia like those that occur during walking, suggesting that they could also be proprioceptive (**Figure 2.1C**). Intracellular recordings from second-order neurons have identified distinct pathways for proprioceptive and vibration sensing, but in some cases also revealed complex pooling of signals from multiple FeCO subtypes[25,26].

Here, we use the FANC[27] and Flywire[8] connectome datasets to reconstruct and analyze neural circuits downstream of the FeCO of the fly's front left (T1L) leg. We find that position- and movement-encoding claw and hook neurons are primarily proprioceptive and connect to local circuits within the VNC for leg motor control. In contrast, vibration-encoding club neurons connect to intersegmental and ascending circuits that integrate mechanosensory information from the legs, wings, and neck, and relay it to the brain. Then, by identifying these ascending projections within the brain, we confirm that this leg vibration information is relayed to auditory circuits downstream of the antenna. We also identify sparse pathways that mediate interactions between proprioceptive and exteroceptive circuits, revealing how vibration signals may directly influence motor output. Overall, our analyses suggest that the FeCO supports both proprioceptive and exteroceptive functions, which are achieved via specialized somatosensory neurons connected to specialized downstream circuits.

2.3 Results

Reconstruction and identification of FeCO axons in the FANC connectome

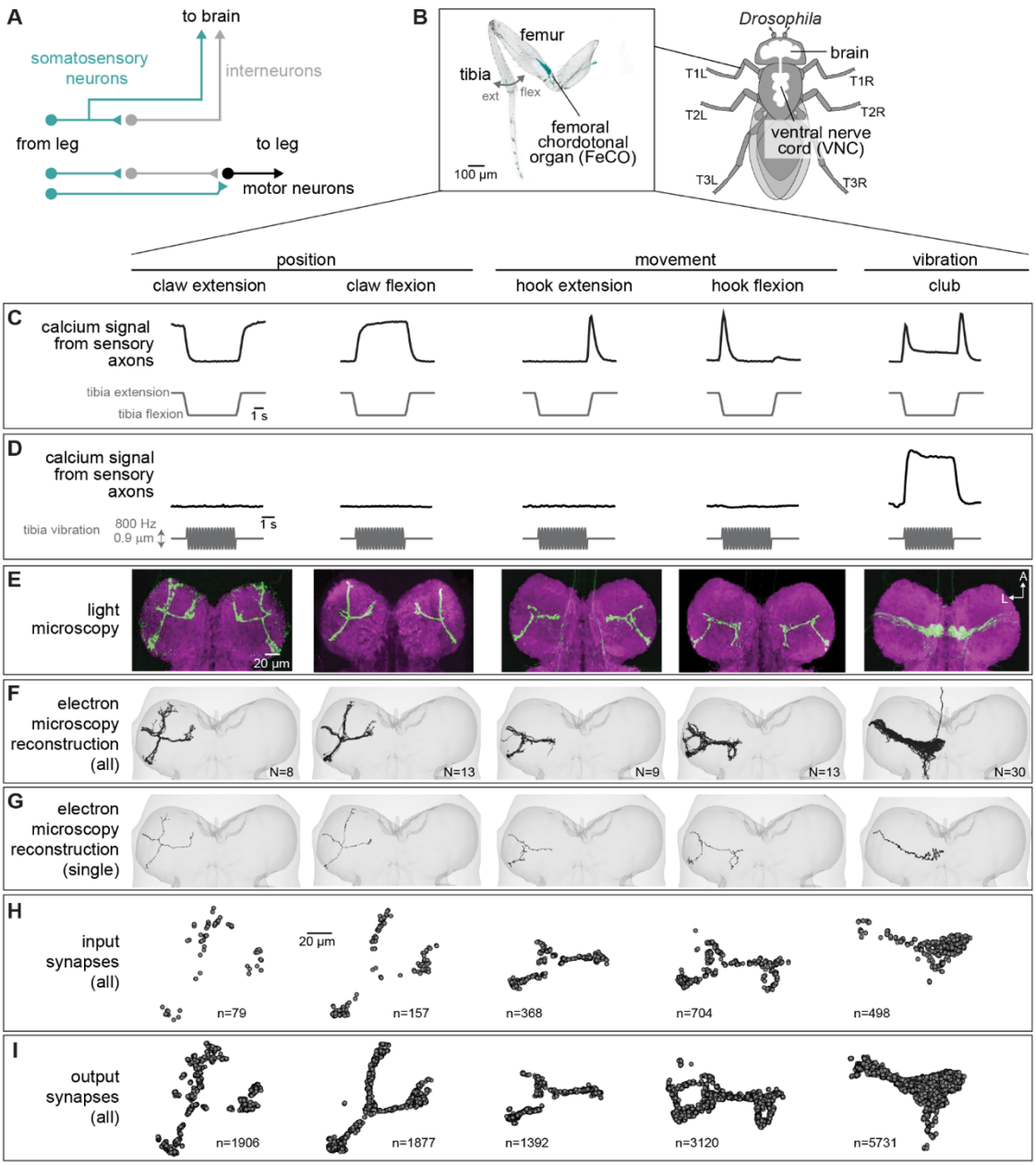

Figure 2.1. Connectomic reconstruction of axonal projections from somatosensory neurons in the femoral chordotonal organ (FeCO) of a female *Drosophila*. (**A**) Schematic of local and ascending VNC circuits for leg somatosensation and motor control. (**B**) Left: Confocal image of a *Drosophila* front leg showing the location of FeCO cell bodies and dendrites. Green: GFP; gray: cuticle auto-fluorescence. Right: Schematic showing the fly brain and ventral nerve cord (VNC) (C-I) Anatomical and functional subtypes of somatosensory neurons in the *Drosophila* FeCO. (**C**) Calcium signals from FeCO axons of each subtype (GCaMP, black traces) in response to a controlled movement of the femur-tibia joint (gray traces). Adapted from Mamiya et al., (2023). (**D**) Calcium signals from FeCO axons of each subtype (GCaMP, black traces) in response to an 800 Hz vibration of the femur-tibia joint (gray traces). Adapted from Mamiya et al., (2023). (**E**) Confocal images of the axons of each FeCO subtype in the fly ventral nerve cord (VNC). Green: GFP; magenta: neuropil stain (nc82). Adapted from Agrawal et al., (2020) A: anterior; L: lateral. (**F**) Reconstructed FeCO axons from each subtype in the front left leg neuromere of the FANC connectome (from left to right, N=8, 13, 9, 13, 35 neurons). (**G**) Single reconstructed axons from each FeCO subtype in the front left leg neuromere of the FANC connectome. (**H**) Locations of all input synapses received by each FeCO subtype (i.e. postsynaptic sites). n indicates the number of synapses. (**I**) Locations of all output synapses made by each FeCO subtype (i.e. presynaptic sites). n indicates the number of synapses.

Using software for collaborative proofreading and visualization of the segmented FANC EM dataset (see Methods), we reconstructed the anatomy and synaptic connectivity of roughly half the FeCO axons from the front left leg (78 total axons, **Figure 2.1F-I**). We focused our reconstruction efforts on these FeCO axons because they project to the front left neuromere of the VNC (also referred to as left T1 or T1L), the region of the *Drosophila* VNC with the most complete information about leg sensorimotor circuits. All of the motor neurons controlling the muscles of the front left leg and their presynaptic partners have been previously identified and reconstructed in FANC[27,28], and prior neurophysiological recordings of FeCO axons and their downstream targets were made in the same region[15,16,25,26,29,30]. Unfortunately, leg sensory axons are among the most difficult neurons to reconstruct in the available VNC connectomes, likely due to rapid cell-death that begins when the legs are separated from the VNC during sample preparation. Although our dataset is missing some FeCO axons, we found that the number of novel postsynaptic partners decreased as we added more axons to the dataset (**Figure S2.1**), suggesting that our reconstruction covers the major components of the postsynaptic circuitry.

The FeCO consists of five functional subtypes that encode tibia position (extension/flexion), directional movement (extension/flexion), and bidirectional movement/vibration (**Figure 2.1C-D**)[20]. We sorted the reconstructed FeCO axons in the connectome into these functional subtypes based on axon morphology and comparison with light microscopy images (**Figure 2.1E-G**; see Methods). Based on an X- ray reconstruction of the peripheral cell bodies[15], we estimate that we reconstructed ~50% of the T1L axons of each subtype: 8 claw extension, 13 claw flexion, and 9 hook extension axons (of ~58 axons), 13 hook flexion axons (of ~28 axons), and 35 club axons (of ~66 axons). Overall, EM reconstructions of axons from each subtype resemble light-level images of FeCO axons[16], including 5 club axons from the

T1L leg that send an ascending projection to the brain. A few FeCO axons, however, demonstrate unexpected within-type diversity, including axons with shortened or doubled branches (**Supplemental Table 2.1**). As expected for sensory neurons, all FeCO axons have more presynaptic sites (i.e., output synapses) than postsynaptic sites (i.e. input synapses) (**Figure 2.1H-I**). Generally, the locations of pre- and postsynaptic sites are intermingled; FeCO axons do not have distinct pre- and postsynaptic zones.

Claw and hook (but not club) axons provide feedback to local leg motor circuits

To investigate pathways downstream of the different FeCO subtypes, we reconstructed the anatomy and synaptic connectivity of all postsynaptic partners that receive at least 4 synapses from a FeCO axon, a threshold used by previous studies[8,31,32]. We classified all postsynaptic VNC neurons into six morphological classes (see Methods): local neurons located entirely in the T1L neuromere: (1) interneurons, (2) motor neurons, (3) sensory neurons, (4) descending and (5) ascending neurons that connect the brain and VNC, and (6) intersegmental neurons, which span multiple VNC neuromeres (**Figure 2.2A**). We interpret connectivity of FeCO axons with local interneurons or leg motor neurons as suggesting a role in local, rapid feedback control of leg motor output. In contrast, we interpret connectivity with ascending neurons as suggesting a role in mediating sensation and behavior on longer timescales, such as sensory perception and action selection.

We found that the majority of synapses from claw and hook extension axons are onto local VNC interneurons and leg motor neurons (**Figure 2.2B, C**). In contrast, more than half of all synapses from club axons are onto intersegmental neurons. Hook flexion axons are somewhere in between, making roughly similar proportions of their synapses onto local and intersegmental

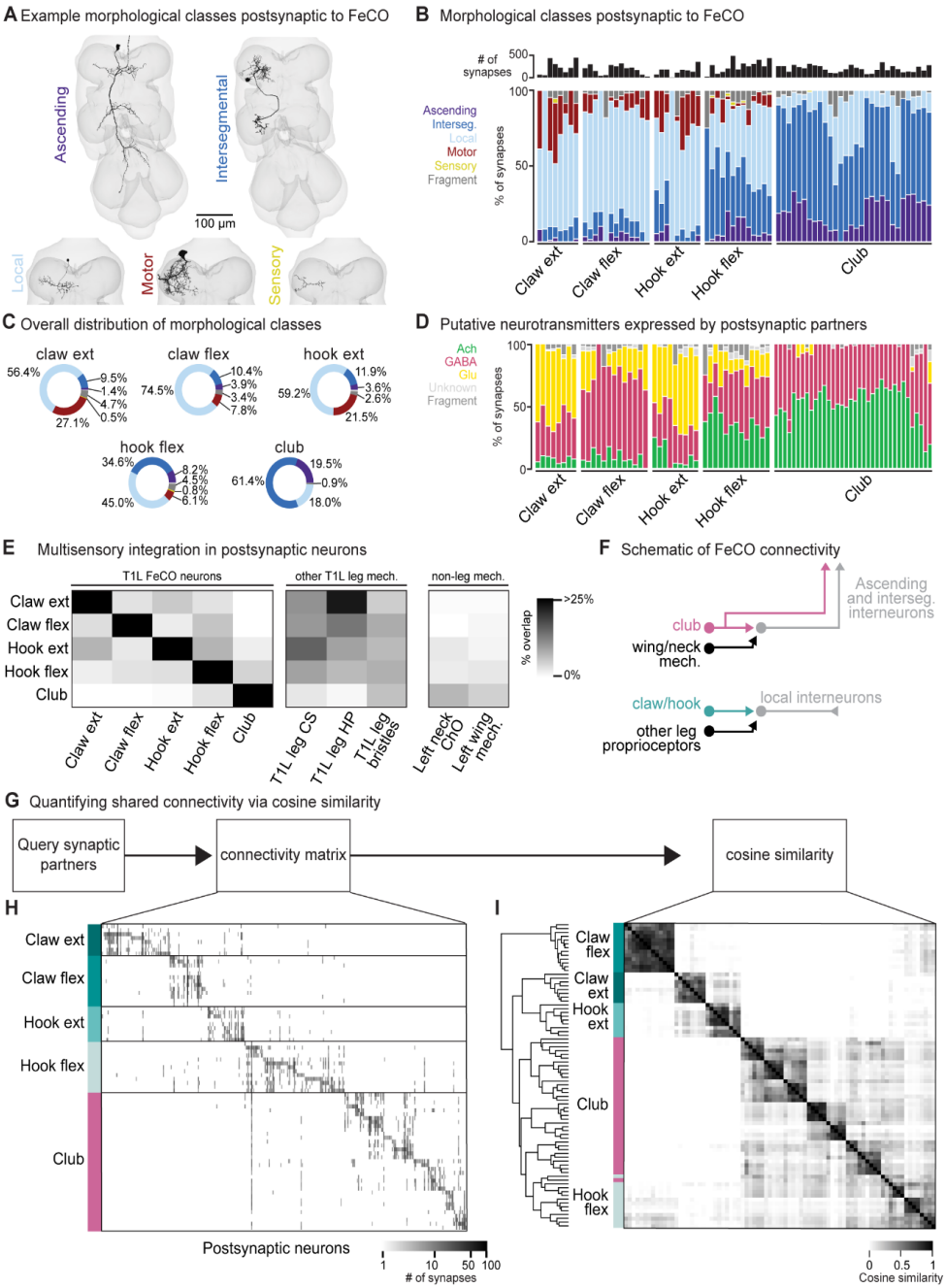

Figure 2.2. FeCO neurons exhibit subtype-specific postsynaptic connectivity. (**A**) We reconstructed all VNC neurons postsynaptic to FeCO axons from the front left leg (T1L) and classified them into morphological classes. Example provided from each class. (**B**) Percent of synapses from each FeCO axon that are made onto VNC neurons of each morphological class. Top bar plot shows the total number of output synapses made by each FeCO axon. (**C**) Per FeCO subtype, the total fraction of output synapses made onto each morphological class. (**D**) Proportion of total synapses made by each FeCO neuron onto cholinergic (green), glutamatergic (yellow), GABAergic (pink), and unidentified (light gray) hemilineages. (**E**) Heatmap shows the percent of neurons postsynaptic to a particular T1L FeCO subtype (as indicated along the rows) that also receive synaptic input from an alternate somatosensory population: T1L FeCO neurons, including claw extension axons, claw flexion axons, hook extension axons, hook flexion axons, or club axons, other T1L leg mechanosensory neurons, including campaniform sensilla axons (CS), hairplate axons (HP), or bristle axons, and non-leg mechanosensory neurons, including left neck chordotonal organ axons or left wing somatosensory axons. We found that neurons postsynaptic to claw and hook axons also integrate information from other leg proprioceptors such as HP axons and CS axons. In contrast, neurons postsynaptic to club axons do not integrate information from other leg proprioceptors, but they do integrate information from wing and neck somatosensory axons.

Fig. 2 legend contd. (**F**) Schematic of FeCO connectivity. Club information is conveyed primarily to ascending and intersegmental neurons, who also receive information from wing and neck somatosensory neurons. Information from claw and hook axons is primarily relayed to local interneurons, which also receive information from other leg proprioceptive neurons. (**G**) By querying the connectivity of each postsynaptic partner of each reconstructed FeCO neuron, we obtained **H**) a connectivity matrix and **I**) a cosine similarity matrix. (**H**) Connectivity matrix between FeCO axons and postsynaptic VNC neurons. The shading of each tick indicates the number of synapses from each FeCO axon (row) onto each postsynaptic VNC neuron (column). Colored bars along the left indicate the presynaptic FeCO subtype for that row. FeCO axons are organized by morphological subtype and then by their cosine similarity scores. VNC neurons are organized by their cosine similarity scores. (**I**) Clustered pairwise cosine similarity matrices of all FeCO axons based on their postsynaptic connectivity. The cosine similarity between two neurons is the dot product of the normalized (unit) column weight vectors. If two FeCO neurons synapse with similar synaptic weights onto the same postsynaptic neuron, relative to the FeCO's total output, the pairwise cosine similarity is 1. FeCO neurons with similar postsynaptic connectivity patterns cluster together, forming connectivity clusters.

postsynaptic partners. Club and hook flexion axons also make a notably high number of synapses onto ascending neurons that convey leg somatosensory information to the brain.

We next used anatomical criteria to identify the developmental origins of all pre- and postsynaptic partners of FeCO axons (see Methods). About 95% of adult neurons in the *Drosophila* VNC arise from 30 segmentally repeated neuroblasts (neural stem cells), each of which divides to form an 'A' and 'B' hemilineage[33]. Developmental hemilineages are an effective means to classify VNC cell types: neurons of the same hemilineage release the same primary neurotransmitter[34] and express similar transcription factors[35,36]. Previous research also suggests that neurons within a hemilineage are functionally related: thermogenetic activation of single hemilineages drove coordinated movements of legs or wings[37], and connectome analyses of larval VNC neurons demonstrated that neurons within a hemilineage share common synaptic partners[38].

We found that club axons target neurons from different hemilineages than claw and hook axons (**Figure S2.2**). Neurons that are primarily postsynaptic to club axons come from hemilineages 8B, 10B, 23B, 0A/0B, 1B, and 9A. Of those, only 1B and 9A neurons receive any synaptic input from claw axons, but the connectivity is weak (~6.34% and 0.46% of total FeCO input, respectively). Club and hook flexion axons target some shared hemilineages, including 23B, 1B, and 9A. Neurons from all other identified hemilineages are predominantly postsynaptic to claw or hook axons and do not receive any synaptic input from club axons. We further used the

hemilineage designations to infer a neuron's likely primary neurotransmitter (**Figure 2.2D**). The majority of *Drosophila* neurons release one of three primary neurotransmitters: acetylcholine, GABA, or glutamate[35,39]. In the fly, acetylcholine is typically excitatory, while GABA is typically inhibitory[35,40,41]. Glutamate is excitatory at the fly neuromuscular junction, acting on ionotropic glutamate receptors (GluRs), but is frequently inhibitory in the CNS, acting on the glutamate-gated chloride channel, GluCl[42]. Club axons synapse onto very few putative glutamatergic neurons (**Figure 2.2D**) compared to claw and hook axons.

We conducted similar analyses examining the presynaptic inputs to FeCO axons (**Figure S2.3**). Generally, hook axons receive the most input synapses and have the most presynaptic partners, which include local, ascending, and intersegmental neurons (**Figure S2.3A, B**). The majority of input synapses to FeCO axons are GABAergic (**Figure S2.3D**). The strongest input comes from 9A neurons, which are primarily presynaptic to hook axons (**Figure S2.3C-D**). Recent work found that a subset of 9A neurons suppress expected proprioceptive feedback during voluntary movement such as walking or grooming[30].

Together, these differences in postsynaptic connectivity suggest that claw and hook axons are connected to postsynaptic partners that are distinct from those downstream of club axons. These downstream partners differ in their morphology as well as their developmental stem-cell lineage. Hook and claw axon connectivity with local and motor neurons suggests that they play a role in fast feedback control of leg motor output. In contrast, club axons connect to intersegmental and ascending pathways that could relay leg vibration information to the brain to support detection of external mechanosensory signals. (**Figure 2.2F**). In support of this conclusion, we found that the neurons that receive input from claw and hook axons also receive input from other leg proprioceptors, such as hair plate and campaniform sensilla neurons, whereas the VNC neurons

that receive input from club axons receive input from somatosensory neurons on the neck and wing, not on the leg (**Figure 2.2E, F**).

FeCO axons demonstrate subtype-specific downstream connectivity

We next investigated the specific postsynaptic partners targeted by claw, hook, and club axons and the degree to which FeCO axons synapse onto distinct or overlapping circuits. First, we constructed a connectivity matrix to look at the postsynaptic connectivity of each FeCO neuron, organizing the rows of the matrix by FeCO subtype (**Figure 2.2G, H**). Generally, postsynaptic connectivity is sparse, with each FeCO neuron contacting only about 21.1 ± 1.1 (mean ± s.e.m.) distinct postsynaptic partners. To quantify this connectivity structure, we calculated the cosine similarity score for pairs of FeCO axons based on their synaptic outputs (**Figure 2.2I**; see Methods). Two FeCO axons have a high cosine similarity score if they make the same relative number of synapses onto the same postsynaptic neurons. Low similarity scores indicate either that two FeCO axons share few postsynaptic partners or that the relative number of synapses onto common postsynaptic partners are different.

Hierarchical clustering of cosine similarity scores confirmed that FeCO axons of the same subtype provide similar synaptic output to the same postsynaptic partners (**Figure 2.2I**). FeCO axons tuned to different tibia positions (claw flexion vs. claw extension axons) or movement directions (hook flexion vs. hook extension axons) demonstrate very low (almost zero) cosine similarity scores, indicating that their postsynaptic connectivity is very different. Instead, hook and claw axons that share directional selectivity (claw and hook flexion or claw and hook extension axons) demonstrate some shared connectivity, as suggested by cosine similarity scores above zero. Unexpectedly, we found that hook flexion axons and club axons share some postsynaptic connectivity, as demonstrated by their relatively high cosine similarity scores and co-clustering.

We also calculated and clustered the similarity scores for FeCO axons based on their synaptic inputs (**Figure S2.3E, F**). However, because FeCO axons have far fewer (and in some cases zero) presynaptic partners (2.9 ± 0.3 neurons, mean ± s.e.m.), these similarity scores are dominated by the shared connectivity of just a few presynaptic neurons. Claw extension and claw flexion axons receive little shared synaptic input. In contrast, hook flexion and hook extension axons all receive very similar synaptic input. Only a small number of club axons receive presynaptic input, but those that do exhibit high similarity to one another, except for two club axons whose upstream connectivity is more similar to that of hook axons.

In summary, FeCO axons demonstrate subtype-specific pre- and postsynaptic connectivity. FeCO axons within a subtype are generally more similar in their connectivity than FeCO axons of different subtypes, suggesting that information from each subtype is conveyed in parallel to different downstream neurons.

Claw and hook axons connect directly and indirectly to leg motor neurons

Thus far, we have found that club axons synapse on VNC neurons from different morphological classes and developmental hemilineages than the claw and hook axons. This segregated connectivity suggests that signals from club neurons are relayed to distinct downstream circuits with different functions than claw and hook neurons. Given that club neurons are the only subtype that respond to low amplitude, high frequency vibration, we hypothesized that this distinct connectivity could reflect an exteroceptive function of club neurons compared to the proprioceptive function of claw and hook neurons. To explore this hypothesis, we next examined how each FeCO subtype connects to leg motor circuits.

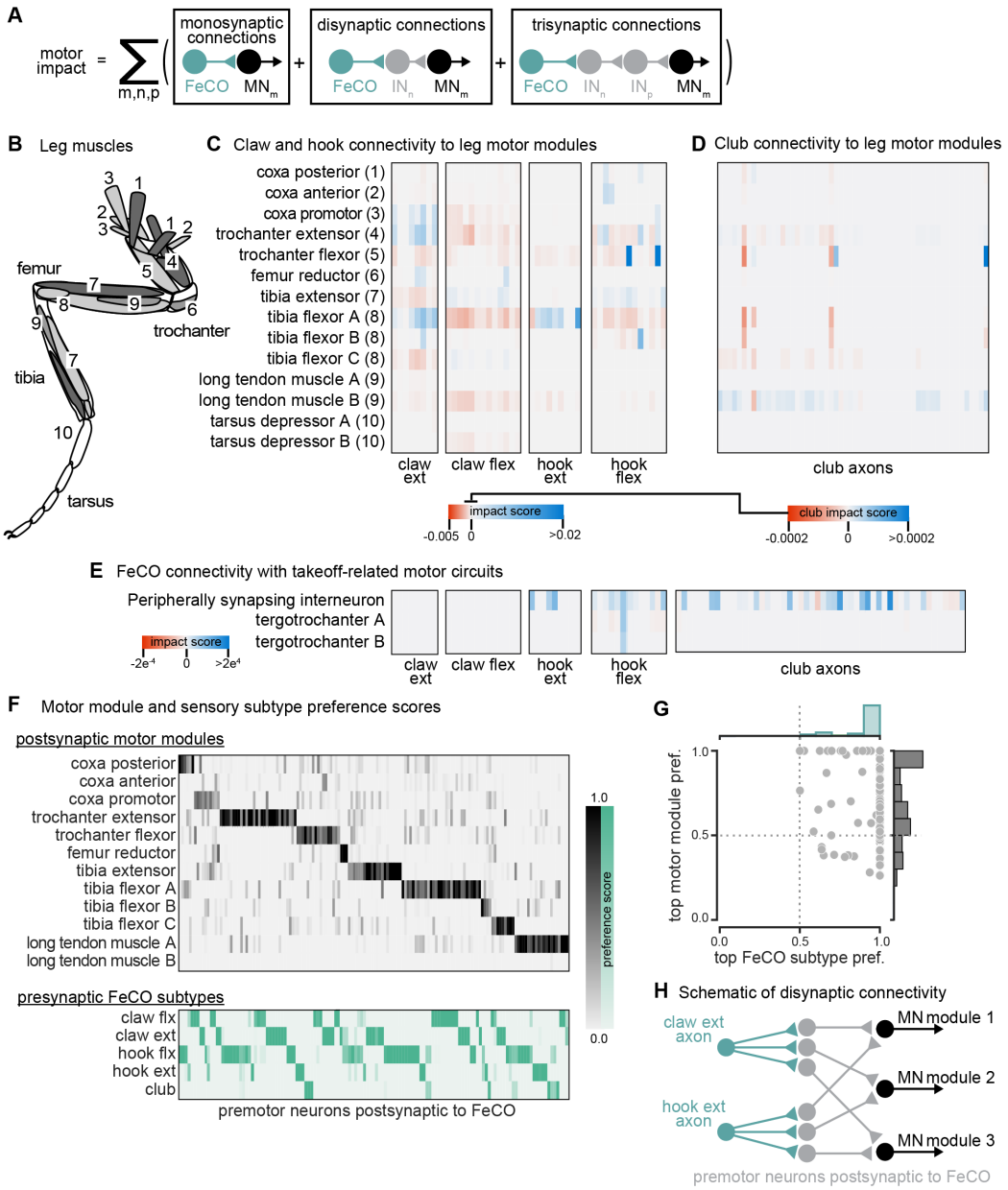

Figure 2.3. The connectivity of hook and claw neurons is structured to impact activity of leg motor neurons. (**A**) We developed an impact score that takes into account monosynaptic, disynaptic, and trisynaptic connections between FeCO axons and leg motor neurons (see methods). (**B**) Schematic of the 18 muscles controlling the fly's front leg. Numbers correspond to motor module labels in panel C. (**C**) Motor impact scores of claw and hook axons on leg motor modules. Motor modules are functional groupings of motor neurons that receive common synaptic input and act on the same joint[27]. The target muscles of each motor module are indicated in panel B. (**D**) Motor impact scores of club axons on leg motor modules. Note the scale bar change from panel C. (**E**) Motor impact scores of FeCO axons onto take-off related motor circuits. The peripherally synapsing interneuron is a premotor neuron involved in takeoff. The tergotrochanter is a leg muscle that is not active during walking but is instead involved in jumping and takeoff [26,43,44]. (**F**) Motor module preference scores (gray, top) and FeCO subtype preference scores (green, bottom) for each premotor VNC neuron that receives input from FeCO axons (columns). Premotor neurons are arranged according to their preferred motor module followed by their preferred FeCO subtype. (**G**) Motor module preference (y-axis) plotted against FeCO subtype preference (x-axis) for each premotor VNC neuron that receives input from FeCO axons. (**H**) Schematic representation of the predominant connectivity pattern seen between FeCO neurons and motor modules. Premotor neurons postsynaptic to the FeCO are primarily dedicated to relaying information from a particular FeCO subtype to a particular motor module.

Some FeCO axons synapse directly onto motor neurons, but they also indirectly excite or inhibit motor neurons via intervening interneurons. We developed an impact score metric (**Figure 2.3A**) that takes into account both direct and indirect connections between FeCO axons and motor neurons, as well as the putative neurotransmitter predicted by hemilineage assignment (see Methods). We then calculated the motor impact score between each FeCO axon and functional pools of leg motor neurons, called motor modules[27] (**Figure 2.3B, C**). Motor modules contain varying numbers of motor neurons that, based on their presynaptic connectivity patterns, comprise a functional motor pool driving a similar movement (e.g., tibia extension).

Claw and hook neurons make direct and indirect connections with many leg motor neurons (**Figure 2.3C**). The pattern of their connectivity is consistent with previous recordings of motor neuron activity and optogenetic manipulations in *Drosophila*[25,29]. Claw and hook flexion axons provide strong excitatory feedback to motor neurons that extend the tibia and inhibitory feedback to motor neurons that flex the tibia. Claw and hook extension axons provide excitatory feedback to motor neurons that flex the tibia and strong inhibitory feedback to motor neurons that extend the tibia. Claw extension axons also provide excitatory feedback to other motor modules, such as the motor neurons that move the coxa forward (coxa promotor) and extend the trochanter. This connectivity suggests that FeCO feedback supports leg motor synergies that span multiple leg joints.

Consistent with our hypothesis that club neurons do not support local leg motor control, club axon connectivity with leg motor neurons is weak, demonstrated by a low impact score (**Figure 2.3D**, note different scale bar). Club axons form no direct synapses onto leg motor neurons. However, they do indirectly and weakly connect to leg motor neurons innervating the long tendon muscle (LTM) (**Figure 2.3D**), which has been shown to control substrate grip[43]. Club

axons also indirectly connect to the premotor peripherally synapsing interneuron (PSI) (**Figure 2.3E),** which is associated with control of the wing during takeoff[27,44,45]. This connectivity suggests a pathway by which activation of club neurons could lead to startle or escape behaviors, such as freezing and take-off.

Finally, we analyzed the overall organization of FeCO axons' premotor connectivity. We found that all postsynaptic premotor interneurons have a strong preference for a single FeCO sensory subtype and a single MN module (**Figure 2.3F-G**). This organization suggests that fly leg motor circuits are organized according to a "labeled line" structure, with dedicated interneurons connecting a single FeCO subtype with a single motor module (**Figure 2.3H**).

Club connectivity is consistent with a putative tonotopic map of tibia vibration frequency

We next sought to understand how club neurons are functionally organized by further investigating their anatomical projection patterns and postsynaptic connectivity. Among the five subtypes, club axons stood out as having the most variable postsynaptic connectivity patterns. Specifically, club axons separated into subclusters that were more similar to one another than other club axons (**Figure 2.2I**). Past recordings of calcium activity from FeCO neurons in response to vibration of the tibia revealed that club axons are organized tonotopically[15,16]. We therefore wondered whether the connectivity clusters we found in the VNC connectome could represent functional groupings of club axons tuned to similar vibration frequencies.

In support of this hypothesis, we found that the spatial organization of the connectivity subclusters of club axons reflects the tonotopy observed in prior experimental recordings. Club axons cluster into 3 groups based on the cosine similarity of their postsynaptic connectivity (**Figure 2.4A**). These connectivity clusters spatially tile the dorsal-ventral axis (**Figure 2.4B**)

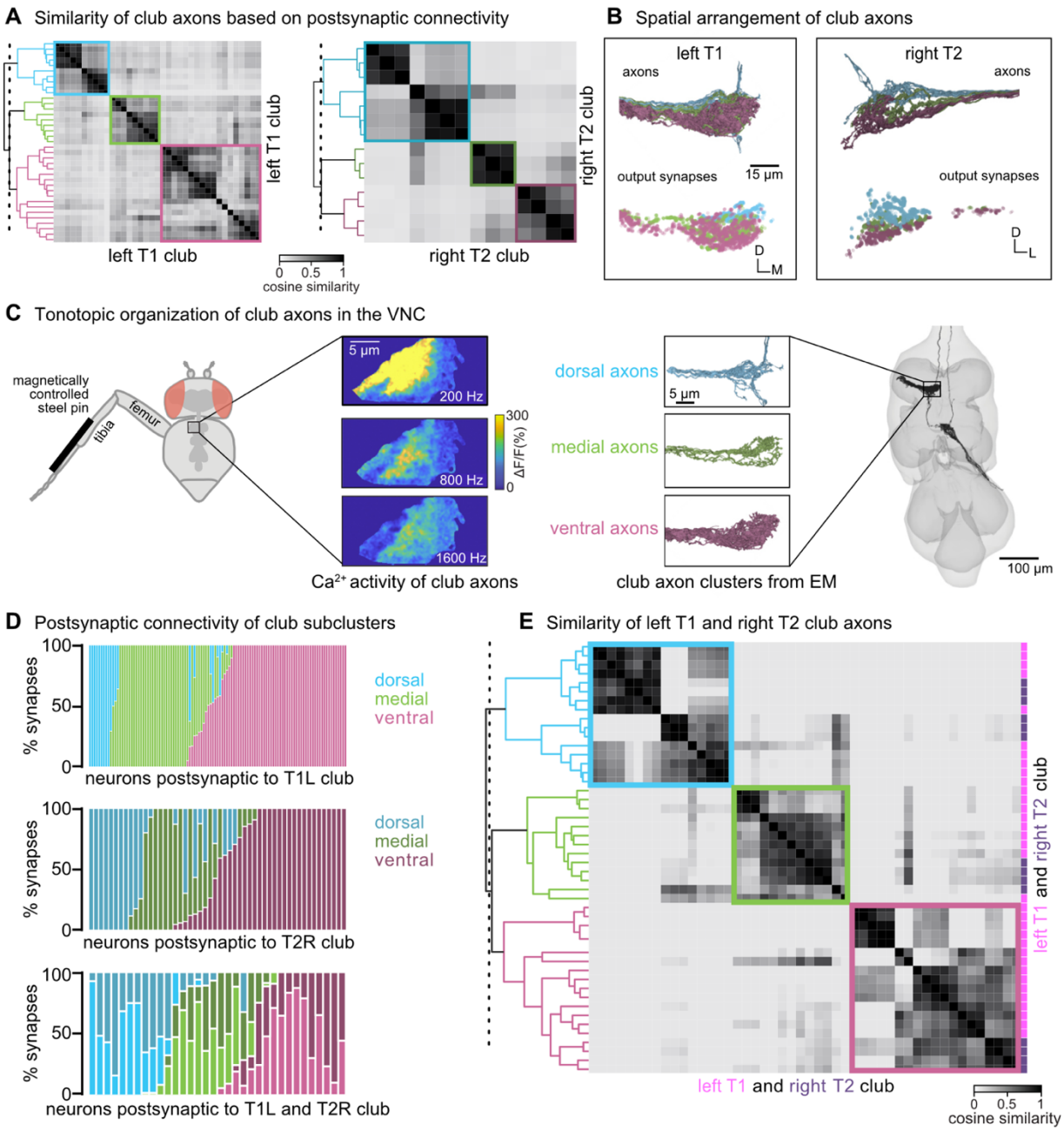

Figure 2.4. Club neurons cluster into spatial groups that reflect the putative tonotopic map of tibia vibration frequency. (**A**) Clustered pairwise cosine similarity matrices of the club axons based on postsynaptic connectivity. Sensory neurons with similar postsynaptic connectivity patterns cluster together, forming connectivity clusters. Left: Matrices for club axons in front left leg with connectivity clusters highlighted in blue (n = 10), green (n = 9), pink (n = 18). Right: Matrices for club axons in the middle right leg (T2R) with connectivity clusters highlighted in blue (n = 7), green (n = 3), pink (n = 4). (**B**) Top, Club axons within each connectivity cluster form 3 groups that span the dorsal-ventral axis: dorsal (blue), medial (green), and ventral (pink). Bottom, the spatial location of the output synapses for each of the club neurons color-coded by the corresponding connectivity cluster. (**C**) The dorsal-ventral organization of connectivity clusters is consistent with tonotopic mapping of tibia vibration frequency recorded from club axons with calcium imaging[15]. Left, Schematic of the experimental set-up. Calcium data from Mamiya et al., (2018) depicting calcium responses from club axons to vibration frequencies (200Hz, 800Hz, 1600Hz) applied to the tibia. Right, reconstructed club axons in the FANC dataset separated by connectivity clusters. (**D**) Fraction of input synapses from club neurons onto downstream partners. Club neurons are grouped based on connectivity cluster (dorsal: blue, medial: green, ventral: pink). (**E**) Clustered pairwise similarity matrices of the T1L (pink) and T2R (gray) club axons based on shared postsynaptic connectivity. Sensory neurons with similar postsynaptic connectivity patterns cluster together regardless of their leg of origin.

similar to the tonotopic organization seen in calcium imaging of club axons in response to tibia vibration (**Figure 2.4C**)[16]. Accordingly, we hypothesize that the most ventral populations are sensitive to lower frequency vibrations, whereas the most dorsal populations (including ascending club axons) are sensitive to higher frequency vibrations. To determine whether this spatial organization is replicated in other leg neuromeres, we reconstructed 14 club axons from the middle right leg (right T2). Club axons from this leg also separate into three spatially distinct subclusters that span the dorsal-ventral axis (**Figure 2.4A-B**). We also found that VNC neurons postsynaptic to club axons receive most of their input from club axons from the same connectivity cluster (dorsal, medial, or ventral) across multiple legs (**Figure 2.4D**). Club axons in the most dorsal clusters of the left T1 and right T2 legs connect to overlapping downstream partners regardless of their leg of origin. Similarly, axons in the ventral-most cluster connect to overlapping downstream partners. Thus, irrespective of the leg of origin, club axons cluster based on their dorsal-ventral organization (**Figure 2.4E**).

In summary, we found that club axons form subclusters that tile the dorsal-ventral axis and share postsynaptic partners. We propose that individual club neurons are spatially clustered along the dorsal-ventral axis based on similarities in vibration frequency tuning. The putative tonotopic structure observed in club axons is preserved in postsynaptic neurons.

Interneurons postsynaptic to club axons integrate information across legs

Club axons primarily synapse onto ascending and intersegmental interneurons (**Figure 2.2**). These downstream neurons are positioned to integrate vibration information across multiple legs, perhaps to enable the fly to detect and localize external vibrations (**Figure 2.5A**). We next investigated the structure of this putative downstream integration by analyzing the circuitry

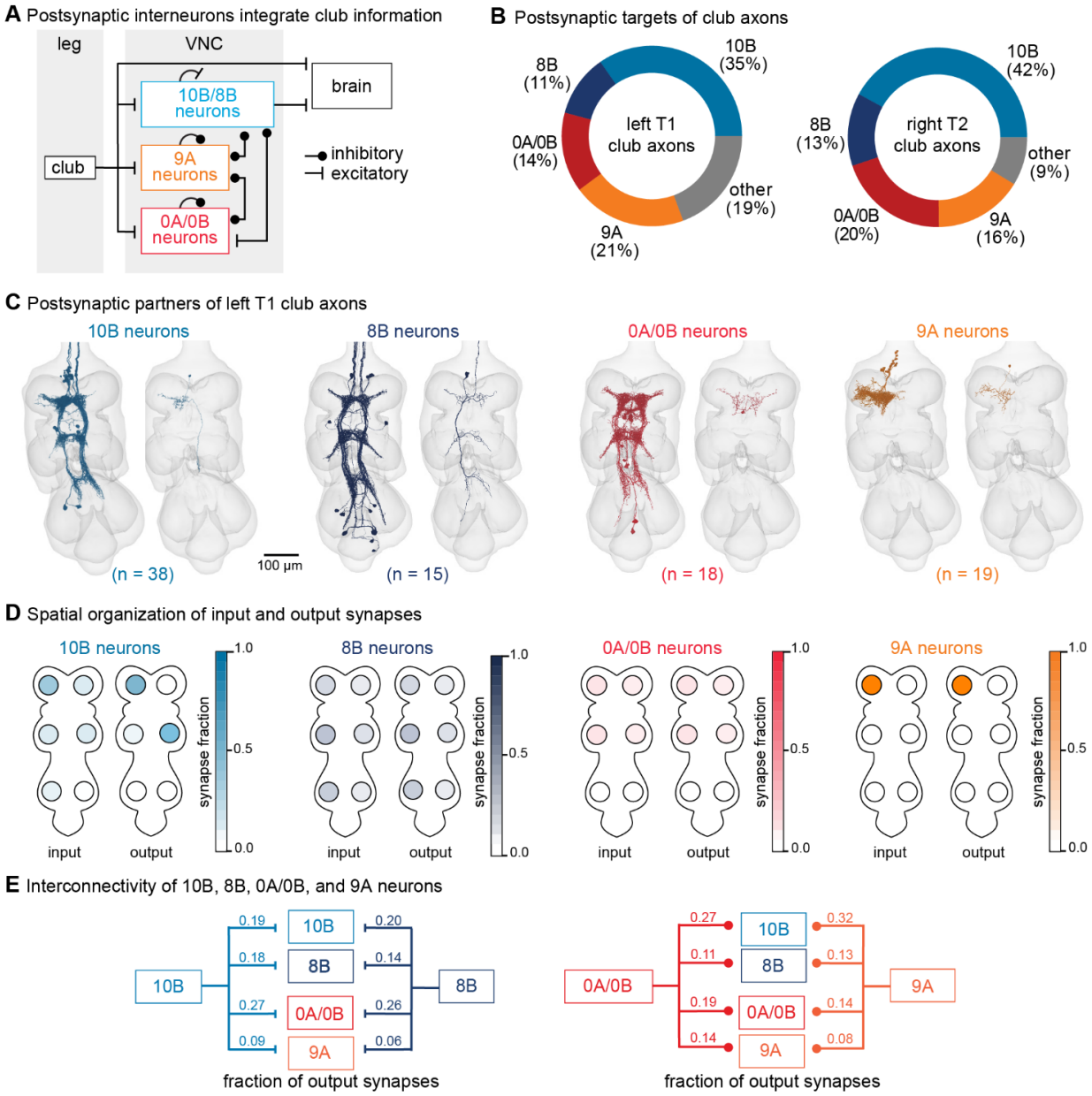

Figure 5. VNC neurons integrate vibration signals from club neurons across multiple legs. (A) Schematic of the multi-layered connectivity downstream of club axons. (B) Fraction of total output synapses from club neurons onto downstream interneurons separated by hemilineage class. 10B (light blue, n = 38), 8B (dark blue, n = 15), 0A/0B (red, n = 18). 9A (orange, n = 19) (C) Reconstructed interneurons downstream of left T1 club neurons from the FANC dataset. Left image shows all reconstructed neurons of a given hemilineage that are downstream of T1L club neurons. Right image shows a single example neuron from that hemilineage. (D) Heatmap depicting the spatial locations of input (left) and output (right) synapses for 10B, 8B, 0A/0B, and 9A interneurons that are downstream of T1L club neurons. (E) Circuit diagram depicting recurrent connections between 10B, 8B, 0A/0B, and 9A interneurons. Each line indicates an excitatory or inhibitory connection and is labeled with the fraction of total output synapses each interneuron class makes with another interneuron class.

postsynaptic to club axons. In addition to reconstructing the interneurons directly downstream of club neurons, we also reconstructed a subset of third order interneurons.

The major downstream partners of club neurons include 8B, 10B, 0A/0B, and 9A neurons (**Figure 2.5B**). These neurons express different primary neurotransmitters – 8B and 10B are cholinergic, whereas 0A/0B and 9A are GABAergic. They also possess distinct morphologies that imply specialized roles in transforming club information **(Figure 2.5C-D)**. Individual 10B neurons primarily receive input from one leg and project to the contralateral and adjacent legs, whereas 8B neurons arborize broadly and have mixed input and output synapses in all six neuromeres. 0A/0B neurons project bilaterally and have pre- and post-synaptic sites on both the right and left side of each VNC segment. 9A neurons are the most localized, with their input and output synapses contained within a single neuromere. The diversity of these interneuron morphologies suggests that club information is broadly relayed across the CNS through parallel pathways that integrate club information locally within a leg and globally across multiple legs. Integration of club signals within a leg could be important for amplification while integration across legs could be important for spatial localization of vibration signals. Lateral and disinhibitory circuits may sculpt vibration information, for example via normalization or gain control across the population.

Additionally, 10B, 8B, 0A/0B, and 9A neurons downstream of club neurons exhibit high levels of recurrent connectivity among interneurons from different hemilineages and different legs (**Figure 2.5E**). Overall, the circuitry downstream of club axons is complex, interconnected, and multi-layered. We hypothesize that this highly interconnected circuit architecture supports the fly's capacity to localize substrate vibrations in the external environment.

Leg vibration information integrates with auditory circuits in the brain

Vibration signals from club neurons are relayed to the brain by ascending club sensory axons and ascending 8B and 10B neurons (**Figure 2.6A**). Since the FeCO has been implicated in sensing substrate vibrations for courtship and escape, we hypothesized that leg vibration information carried by the ascending projections is integrated in the brain with other sensory information from the antennae. The fly antenna also contains a chordotonal organ known as the Johnston's Organ, which detects antennal displacements and local air vibrations[46–48]. To this end, we next identified where these ascending neurons project to in the brain and analyzed their downstream connectivity.

Within the FANC connectome, we reconstructed 8 ascending club axons from two legs, 58 ascending 10B neurons, and 52 ascending 8B neurons (**Figure 2.6A**, bottom**)**. We then used a connectome of the fly brain[8,32] to identify ascending projections that matched light-level morphology of ascending projections from club axons, 8B neurons, and 10B neurons (**Figure 2.6A**, top). Within the brain connectome, we found 24 axons that matched the projections of ascending club axons and 94 axons that matched the ascending projections of 8B and 10B neurons. Due to the similarity of their ascending projections, we could not resolve which interneuron axons belonged to which hemilineage (8B or 10B) in the brain connectome. However, 8B/10B branching patterns in the brain are notably different from those of ascending club neurons. Club axons are smooth with few branches, while 10B/8B axons branch extensively.

To understand how the information in these two ascending pathways differs, we compared their connectivity in the VNC and the brain (**Figure 2.6B**). Ascending club axons and 8B/10B neurons are interconnected and share several downstream partners in the VNC. Approximately 30% of output synapses from the ascending club axons are onto ascending 8B/10B interneurons. Additionally, the majority of postsynaptic partners of ascending club axons in the VNC and the

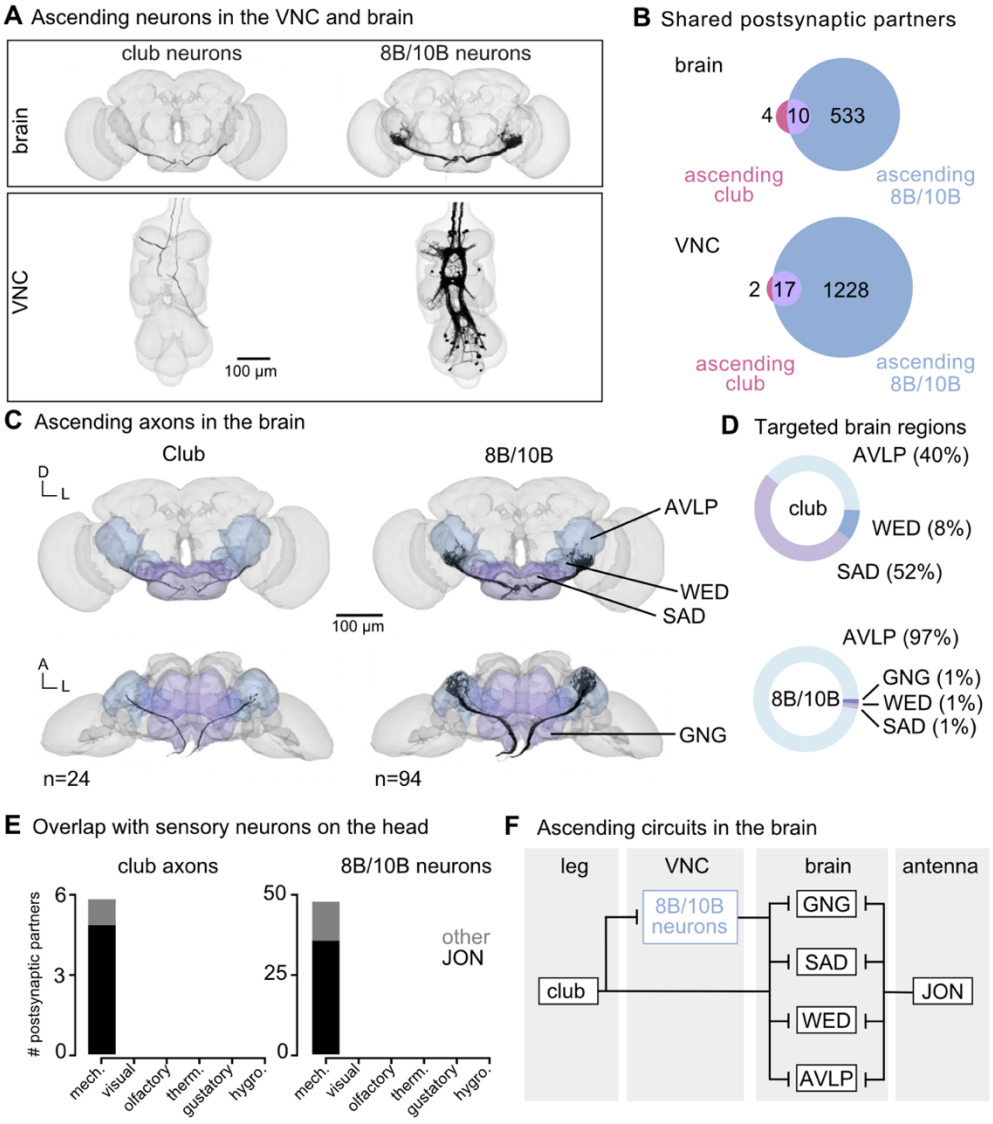

Figure 2.6. Vibration signals from club neurons are transmitted directly and indirectly to the brain and integrated with auditory signals from the antenna. (**A**) Ascending club axons and ascending 8B and 10B interneurons that are reconstructed in the FANC (bottom, 8 club axons and 52 interneurons) and Flywire (top, 24 sensory axons and 94 interneuron axons) datasets. (**B**) Venn diagrams of shared postsynaptic partners between ascending club neurons and ascending 8B/10B neurons in the VNC (top) and brain (bottom). (**C**) Images of the ascending club axons (n = 24) and ascending 8B and 10B interneurons (n = 94) in the brain dataset with targeted brain regions highlighted (Flywire). Axons project to the anterior ventrolateral protocerebrum (AVLP), wedge (WED), saddle (SAD), and gnathal ganglion (GNG). (**D**) Percentage of synaptic outputs from ascending club axons (top) and ascending 8B/10Bs interneurons (bottom) in each brain region. The ascending club axons and ascending interneurons differ with respect to distribution of output synapse location. (**E**) Number of postsynaptic partners of ascending club axons (left) and ascending 8Bs/10Bs (right) that are shared with other sensory neurons in the brain. JON = Johnston's Organ. (**F**) Circuit diagram depicting the projection patterns of ascending club and ascending 8B/10B interneurons in the brain which integrate with antennal auditory circuits.

brain also receive input from ascending 8B/10B interneurons (**Figure 2.6B**). However, 8B/10B neurons have many more postsynaptic partners than club neurons. Thus, 8B/10B neurons target

many of the same postsynaptic partners as ascending clubs, but also contact several non-overlapping downstream partners as well.

Consistent with our hypothesis that club neurons are exteroceptive, we found that ascending club and 8B/10B neurons target known auditory brain regions: the anterior ventrolateral protocerebrum (AVLP), wedge (WED), saddle (SAD), and gnathal ganglion (GNG) (**Figure 2.6C, D**). The AVLP, WED, SAD, and GNG receive integrated auditory information[49] and are responsive to courtship song[50]. Neurons in the WED also respond to antennal vibrations and are tonotopically organized[46]. Across sensory modalities, the ascending club and 8B/10B neurons converge onto shared downstream partners with antennal mechanosensory neurons, namely Johnston's Organ neurons (JONs) (**Figure 2.6E**). This shared connectivity suggests that, in the brain, leg vibration information is compared to mechanosensory information from the antennae. We speculate that this comparison could contribute to the detection and localization of mechanical vibrations in the external environment (**Figure 2.6F**).

2.4 Discussion

Here, we use connectomic reconstruction of neural circuits to infer the function of limb somatosensory neurons from patterns of synaptic connectivity. Our analyses suggest a dual function for the *Drosophila* femoral chordotonal organ (FeCO): position and movement-sensing claw and hook neurons are primarily proprioceptive, providing feedback to local leg motor circuits. In contrast, vibration-sensing club neurons are primarily exteroceptive and provide feedback to intersegmental circuits that integrate somatosensory information across multiple limbs and then convey that information to the brain. Prior experiments in *Drosophila* and other insects had suggested a dual function[16,19–24], but it was previously unknown whether proprioception and exteroception were supported by distinct or overlapping subtypes of FeCO sensory neurons and

downstream interneurons. These analyses demonstrate the power of connectomic mapping and analysis to identify putative functions of somatosensory neurons. They also motivate future work that tests the function of circuits for limb proprioception and exteroception in behaving flies.

Role of the FeCO in local leg motor control

We found that movement- and position-sensing hook and claw axons synapse directly and indirectly onto leg motor neurons (**Figure 2.3**). For example, extension-sensitive claw and hook axons provide excitatory input to the tibia and tarsus flexor motor neurons and inhibitory input to tibia extensor motor neurons. Flexion-sensitive claw and hook axons demonstrate the opposite pattern of connectivity, primarily exciting extensors and inhibiting flexors. This connectivity is consistent with prior evidence that the FeCO contributes to stabilization of leg posture[19,25,29]. Claw and hook axons also provide feedback to motor neurons controlling movement about other joints. Multi-joint, intra-leg feedback from the FeCO has also been found in locusts[51] and wētās[52].

Proprioceptive feedback needs to be flexibly tuned to reflect behavioral demands[53]. For example, during voluntary movement, proprioceptive pathways promoting stabilizing reflexes may be attenuated to avoid opposing the intended movement. One possible mechanism underlying this context-dependent tuning is presynaptic inhibition of sensory axons[54,55]. In support of this mechanism, we found several inhibitory upstream partners of claw and hook axons (**Figure S2.3**). We also showed in a recent study that hook axons are presynaptically inhibited during voluntary movement[30]. In addition to direct feedback onto somatosensory axons, proprioceptive feedback is also likely tuned via context-dependent inhibition of downstream pathways.

Finally, we found that claw and hook axons synapse onto a small number of intersegmental and ascending neurons (**Figure 2.2**). Intersegmental projections could relay proprioceptive

information to the motor circuits of other legs. However, past work suggests that feedback from the FeCO of one leg does not strongly affect control of other legs – manipulating activity of FeCO neurons has little effect on inter-leg coordination[56–58]. One study described intersegmental neural pathways that receive input from the FeCO and mediate reflexes of adjacent legs, though they did not specifically test the effects of manipulating FeCO activity[59]. Ascending neurons that are postsynaptic to claw and hook neurons could relay leg proprioceptive information to the brain to inform motor planning. Calcium imaging experiments have shown that many ascending neurons are active during behaviors like walking[60]. Additionally, visual neurons and neurons within motor planning regions of the fly brain, such as the central complex, encode walking stride, speed, and turning behavior even in the absence of visual input, suggesting that they receive self-motion cues from the legs[61–63].

Tonotopic organization of club axons

Individual club neurons are tuned to specific vibration frequencies, collectively forming a tonotopic map in the VNC[20,64]. We found that club axons are spatially organized into sub-clusters with shared postsynaptic connectivity that tile the dorsal-ventral axis of the VNC (**Figure 2.4**). By comparing this spatial organization to prior recordings of club axon activity in the VNC[64], we hypothesize that the most dorsal club axons respond to higher frequencies while the most ventral club axons respond to lower frequencies. While all club neurons synapse onto ascending interneurons, only the most dorsal club axons ascend directly to the brain. Thus, we predict two pathways for club information to reach the brain: 1) a direct sensory pathway that carries high-frequency vibrations from the legs and 2) an indirect pathway that carries tonotopically organized and spatially localized vibration information. High-frequency information may be particularly

salient, necessitating a more rapid behavioral response compared to broadband vibrations. Vibration sensing is an important yet understudied sensory modality in insects and other animals[65]. For example, recent evidence from mice shows that auditory and high-frequency tactile vibration signals converge in the inferior colliculus and are used to avoid mechanically vibrating environments[66].

Putative exteroceptive function of club neurons

Our analysis of the connectome supports the hypothesis that club neurons primarily function as vibration-sensing exteroceptors. Insects utilize substrate vibrations for social communication, predator detection, and environmental sensing, such as wind[67]. Many insect species possess subgenual organs, specialized vibration sensors in the tibia, but flies and beetles lack these sensory structures[67]. Thus, club neurons may be the primary sensors for detecting substrate vibrations in the fly leg. Previous studies across multiple insect species have implicated the FeCO in escape and courtship responses[21,23,24]. Crustaceans also have leg chordotonal organs that can detect both joint movement and external substrate vibrations, with reported involvement in detecting vibration-based social communications[68–70].

In *Drosophila,* courtship song involves both airborne and substrate-borne vibrations. Males vibrate their wings, producing an airborne "song" that is detected by females via the antennae[71–74]. Males also tap their abdomens, producing substrate-borne vibrations that promote pausing in females[75]. Genetic silencing of FeCO neurons in female flies reduces their receptivity to male courtship song[23], suggesting that the FeCO is involved in courtship. Consistent with this hypothesis, we found downstream neurons in the brain that integrate vibration information from both legs and antennae (**Figure 2.6**). Vibration-sensitive JONs and club neurons respond to

overlapping vibration frequency ranges applied to the antenna or leg, respectively[20,46–48,64], but the full sensitivity range for each group has not been carefully measured. We hypothesize that the integration of vibration information from the antennae and legs could inform courtship behavior by providing overlapping information regarding both airborne and substrate-borne courtship communication. Importantly, in this study, we reconstructed the FeCO circuits within a female VNC. If club neurons are involved in detecting courtship-related signals, the circuitry downstream of the club neurons could be sexually dimorphic and thus different in male flies.

Aside from courtship, vibration information from club neurons could be used for detecting movements of predators or other threats, such as wind or rain. Consistent with this hypothesis, we found that club axons are indirectly connected to escape-related neurons, namely the motor neurons innervating the long tendon muscle (LTM) and the premotor peripherally synapsing interneuron (PSI) (**Figure 2.3**). Activation of club neurons could promote leg freezing via activation of the LTM, or take-off via activation of the PSI.

Lack of convergence across FeCO subtypes in second-order neurons

We were surprised to find that the downstream connectivity of each FeCO subtype is quite distinct: very few VNC neurons receive synapses from more than one FeCO subtype (**Figure 2.2**). Past work had proposed a higher degree of convergence across FeCO subtypes. Using whole cell patch-clamp recordings and 2-photon calcium imaging, one study found multiple VNC interneuron cell types that encode combinations of femur-tibia joint movement, position, and vibration, suggesting that they receive input from multiple FeCO subtypes[25]. Another combined optogenetic activation and calcium imaging to directly map the functional connectivity between FeCO axons and their downstream partners[26]. That study also found examples of VNC interneurons that receive

inputs from more than one FeCO subtype. One possible explanation for this discrepancy is that our connectomic analyses predominantly focused on direct connections between FeCO neurons and their synaptic partners. The integration of information from multiple FeCO subtypes could be via indirect connections involving multiple intervening interneurons. In addition, Agrawal et al., (2020) found strong evidence for gap junctions that connect FeCO sensory neurons with some downstream partners. The FANC EM dataset was not imaged at sufficient spatial resolution to resolve electrical synapses. Finally, we did find some weak shared connectivity between FeCO cell types that share directional selectivity, such as claw and hook flexion axons or claw and hook extension axons. Due to the adventitious nature of their physiology experiments, Agrawal et al., (2020) and Chen et al., (2021) may have, by chance, characterized the few interneurons that do indeed receive synaptic information from multiple FeCO subtypes.

We did find, however, substantial overlap in the downstream connectivity of FeCO neurons and other leg proprioceptive neurons, such as campaniform sensilla (CS) and hairplates (HP) (**Figure 2.2E**). In fact, claw and hook axons shared a larger number of downstream partners with CS or HP neurons than with other FeCO subtypes. Work from stick insects and other models suggest that such multimodal input is important for context-dependent control of proprioceptive reflexes[76,77]. For example, signals from load-sensing CS neurons can reduce the effect of FeCO activation on leg motor neurons.

Although there is no overlap in the downstream connectivity of claw axons or hook extension axons and club axons, we did find some overlap in the connectivity of hook flexion and club axons (**Figure 2.2**). In fact, some club axons share more downstream connectivity with hook flexion axons than with other club axons. This finding is consistent with Agrawal et al., (2020), who found one cell type, 9Aa neurons, that respond to both flexion and vibration of the femur-

tibia joint. However, the implications of this overlap remain to be investigated. For example, such overlap could enable the fly to determine if the source of the vibration is due to movement of its leg. Alternatively, perhaps flies concurrently sense movement and vibration information from the leg to assess substrate texture.

Looking forward

Connectome analysis is a powerful tool to generate and falsify hypotheses about circuit function. Thanks to advances in serial-section electron microscopy and image segmentation, we are close to having multiple connectomes of small model organisms. As more neurons within these connectomes are connected to specific functions, such as motor neurons that control a particular joint or sensory neurons that detect specific signals, these maps become increasingly useful anatomical frameworks for generating hypotheses about the neural control of behavior. Though physiological and behavioral measurements are still necessary in order to determine how a circuit functions, our study illustrates how a global view of synaptic connectivity can reveal organizing principles that motivate future experiments.

2.5 Acknowledgements

We thank members of the Tuthill laboratory for technical assistance and feedback on the manuscript. We also thank Jasper S. Phelps, Wei-Chung Allen Lee, and the FANC community for their contributions to the proofreading of the VNC connectome. We thank Leila Elabaddy, Ellen Lesser, Shirin Mohammadian, Gwendolyn Swannell, and Brandon Pratt for granting us permission to use their unpublished reconstructions of sensory neurons in FANC. We thank Jim Truman, David Shepherd, Haluk Lacin, and Elizabeth Marin for assistance with hemilineage identification.

This work was supported by a Postdoctoral Research Fellowship from the Deutsche Forschungsgemeinschaft (DFG, German Research Foundation) project 432196121 to C.J.D, a Searle Scholar Award, a Klingenstein-Simons Fellowship, a Pew Biomedical Scholar Award, a McKnight Scholar Award, a Sloan Research Fellowship, the New York Stem Cell Foundation, and NIH grants R01NS102333 and U19NS104655 to J.C.T., NIH grants K99NS117657 and R00NS117657 to S.A, and NIH grant T32 NS 99578-3 to S.J.L. and J.C.T.

2.6 Methods

Key resources table

Reagent type (species) or resource	Designation	Source or reference	Identifiers	Additional information
Deposited data	FANC connectome	Azevedo et al. (2022)	https://fanc.community	
Deposited data	FAFB/FlyWire connectome	Dorkenwald et al. (2023, Schlegel et al. (2023)	https://flywire.ai	
Software,	CAVEclient	Dorkenwald et	https://github.co	

algorithm		al. (2023)	m/seunglab/CAVEclient	
Software, algorithm	neuPrint	Plaza et al. (2022)	https://neuprint.janelia.org/	
Software, algorithm	Neuroglancer		RRID:SCR_015631	
Software, algorithm	Python		RRID:SCR_008394	

Reconstruction of neurons in the FANC connectome

Neurons in the Female Adult Nerve Cord (FANC) electron microscopy dataset[9] were previously segmented in an automated manner [27]. To manually correct the automated segmentation of our neurons of interest, we used Google's collaborative Neuroglancer interface[78]. Many of the FeCO axons in T1L were previously identified[9], and most of the claw and hook axons were previously corrected[30]. Here, we identified and corrected additional claw axons as well as all club axons in T1L and T3R. Identification was guided by light-level images of FeCO subtype-specific genetic driver lines[16,20].

To reconstruct pre- and postsynaptic partners of FeCO neurons, we identified all objects in the automated segmentation that received at least 4 synapses from an FeCO neuron or made at least 3 synapses onto an FeCO neuron. We then proofread those objects until associated with either a cell body, or an identified descending or sensory process. A small number of objects were categorized as fragment segments and could not be connected to a cell body or an identified

descending or sensory process. We deemed a neuron as "proofread" once its cell body was attached, its full backbone reconstructed, and as many branches as could be confidently attached. Neuron annotations were managed by CAVE, the Connectome Annotation Versioning Engine[79]. We used custom Python scripts to interact with CAVE via CAVEclient[79].

Novel partners analysis

To identify the number of new postsynaptic partners added to our dataset per each FeCO sensory neuron we reconstructed, we first found all postsynaptic partners of all reconstructed T1L FeCO axons. Then, we randomly sampled the FeCO neurons one at a time (without replacement) in a cumulative fashion, and calculated how many novel postsynaptic partners were connected to each additional FeCO neuron. We re-did this random sampling fifty times.

Cosine similarity scores

Cosine similarity (for example, **Figure 2.2I**) was calculated using the cosine similarity method from the scikit-learn python package. Cosine similarity scores were then hierarchically clustered using the agglomerative clustering methods from the scikit-learn python package.

Definition of cell classes

Neurons pre- and postsynaptic of FeCO axons were identified as motor, sensory, ascending, descending, intersegmental, or local neurons. Motor neurons have a cell body in the VNC and a process in the leg nerve. These neurons were recently identified in the FANC dataset for the front left leg[27,28]. Sensory neurons have a process in the leg nerve but no cell body in the VNC. Ascending neurons have a process in the neck connective and a cell body in the VNC. Descending

neurons have a process in the neck connective but no cell body in the VNC. Intersegmental and local neurons have a cell body and all processes in the VNC. The processes of intersegmental neurons spanned multiple neuromeres, whereas those of local neurons were contained in a single neuromere. All pre- and postsynaptic neurons were manually checked to make sure they were in the correct categories.

Identification of hemilineages

In *Drosophila*, neurons that share a developmental origin (i.e., belong to the same hemilineage) possess common anatomical features[37] and release the same fast-acting neurotransmitter (e.g. GABA, glutamate, or acetylcholine)[34]. We took advantage of this knowledge to identify the hemilineage of each neuron upstream and downstream of FeCO axons in the FANC connectome. We first identified and grouped together local, intersegmental, and ascending VNC neurons based on where their primary neurite entered into the neuropil. These groups of similar primary neurites were then identified as known hemilineages using light microscopy images of sparse GAL4 lines, cell body position along the dorsal-ventral axis[34,37,80,81], and personal communication (James W. Truman, David Shepherd, Haluk Lacin, and Elizabeth Marin). Putative neurotransmitter was then assigned by referencing Lacin et al., (2019). Not all of the clues are available for all of the neurite bundles. See **Supplemental Table 2** for links to view entire populations of each hemilineage in Neuroglancer, an online tool for viewing connectomics datasets[78].

Motor impact score

A presynaptic neuron's monosynaptic impact score onto a postsynaptic neuron is defined as the number of synapses made by the presynaptic neuron onto the postsynaptic neuron, divided by the

total number of input synapses received by the postsynaptic neuron. Then, based on the presynaptic neurons' putative neurotransmitter according to its hemilineage assignment, this impact score is either considered excitatory (or positive) or inhibitory (or negative). In the fly, acetylcholine is typically excitatory, while GABA is typically inhibitory[35,40,41]. Glutamate is excitatory at the fly neuromuscular junction, acting on ionotropic glutamate receptors (GluRs), but is frequently inhibitory in the CNS, acting on the glutamate-gated chloride channel, GluCl [42].

To compute the motor impact score of a given FeCO neuron onto a motor module (**Figure 2.3**), we summed together the calculated impact scores of direct, monosynaptic connections, disynaptic connections, and trisynaptic connections between the FeCO neuron and all MNs within a module. The impact score of monosynaptic connections between an FeCO neuron and a motor module is as described above but summed across all MNs within a module. We assume that FeCO input to MNs would be cholinergic, and thus excitatory.

For the impact score of a disynaptic connection, we first found all neurons with an identified hemilineage that were postsynaptic to the FeCO neuron and presynaptic to the MNs within the relevant module. We then multiplied the monosynaptic impact score from the FeCO neuron onto one of these postFeCO/preMN neurons by the impact score of the postFeCO/preMN neuron onto the MNs within a module. If the postFeCO/preMN neuron was identified as cholinergic, then this disynaptic impact score was considered to be excitatory/positive, and if it was identified as GABAergic or glutamatergic, then it was considered to be inhibitory/negative. We then summed together all disynaptic impact scores from the FeCO neuron to the MNs of a module.

For the impact score of a trisynaptic connection, we first found all neurons with an identified hemilineage that were postsynaptic to the FeCO neuron (postFeCOs), all neurons with

an identified hemilineage that were presynaptic to the MNs within the relevant module (preMNs), and then only included postFeCO neurons that were presynaptic to a preMN neuron, and preMN neurons that were postsynaptic to a postFeCO neuron. We then multiplied the monosynaptic impact score from the FeCO neuron onto a postFeCO neuron by the impact score of the postFeCO neuron onto a preMN neuron, and this was multiplied by the impact score of the preMN neuron onto the MNs within a module. If both the postFeCO and preMN neurons were excitatory or both inhibitory, then this trisynaptic impact score was positive. If one neuron was inhibitory and one was excitatory, then this trisynaptic impact score was negative. We then summed together all trisynaptic impact scores from the FeCO neuron to the MNs of a module.

Preference score

To compute the preference score for a motor module (**Figure 2.3**), we summed the number of synapses onto each MN within a module (as defined by Lesser et al., 2023) and divided by the total synapses onto all MNs. To compute the sensory subtype preference score for a FeCO subtype (**Figure 2.3**), we summed the number of synapses received from all FeCO neurons of a given subtype and divided by the total synapses received from all FeCO neurons.

Circuit analysis in the FAFB/FlyWire connectome

To study connectivity in the brain, we used the Full Adult Fly Brain connectome (FAFB; (Zheng et al., 2018) reconstructed and proofread by the FlyWire community (Dorkenwald et al., 2023a; Schlegel et al., 2023; Zheng). All data are from public release version 630.

Identification of ascending neurons in FAFB/FlyWire connectome

First, we manually screened through the repository of Gen1 MCFO images on FlyLight [81] for candidate images of VNCs that exhibit hallmark expression of the ascending club axons, ascending 8B interneurons, and ascending 10B interneurons in the VNC. To identify the anatomy of the ascending projections in the brain, we matched the ascending axons and interneurons in the VNC to the corresponding images in the brain. Next, we matched the anatomy of the ascending projections in the brain based on the light-level images to the FAFB dataset using flywire.ai[83] and the Codex platform[84]. Specifically, we queried neurons classified as ascending and cholinergic[85,86], then matched candidates to the light-level images of the target neurons. See **Supplemental Table 3** for links to view the ascending neurons in Neuroglancer[78].

Software and data availability

Data presented in the paper was analyzed from the CAVE materialization v604 timestamp 1684915801.222989. Annotated connectivity matrices (**Figure 2.2**) will be available as python Pandas data frames (https://pandas.pydata.org/) at the git-hub repository: https://github.com/sagrawal/Lee_2024. Also available at the repository are scripts to recreate the analyses and figures in the paper, as well as scripts to recreate the connectivity matrices for users authorized to interact with the CAVEclient. Links to public segmentations are available throughout the text, as well as in a document at the git-hub repository. All analysis was performed in Python 3.9 using custom code, making extensive use of CAVEclient (https://github.com/seung-lab/CAVEclient) and CloudVolume to interact with data infrastructure, and libraries Matplotlib, Numpy, Pandas, Scikit-learn, Scipy, stats-models and VTK for general computation, machine learning and data visualization. Additional code is available at

https://github.com/htem/FANC_auto_recon, providing additional tutorials, code and documentation for interacting with FANC.

2.7 Supplementary Materials

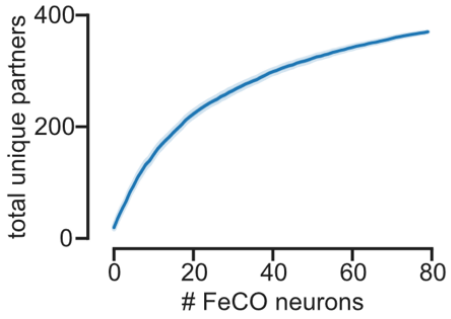

Figure S2.1 Novel partners analysis suggests we have reconstructed a meaningful fraction of the FeCO axons from the front left leg. Plot shows the average number of new postsynaptic partners added to our dataset per each FeCO sensory neuron we reconstructed. We randomly sampled the FeCO neurons one at a time (without replacement) in a cumulative fashion, and calculated how many novel postsynaptic partners were connected to each additional FeCO neuron. We resampled fifty times. Mean (solid line) and standard error (shaded region surrounding line) are plotted.

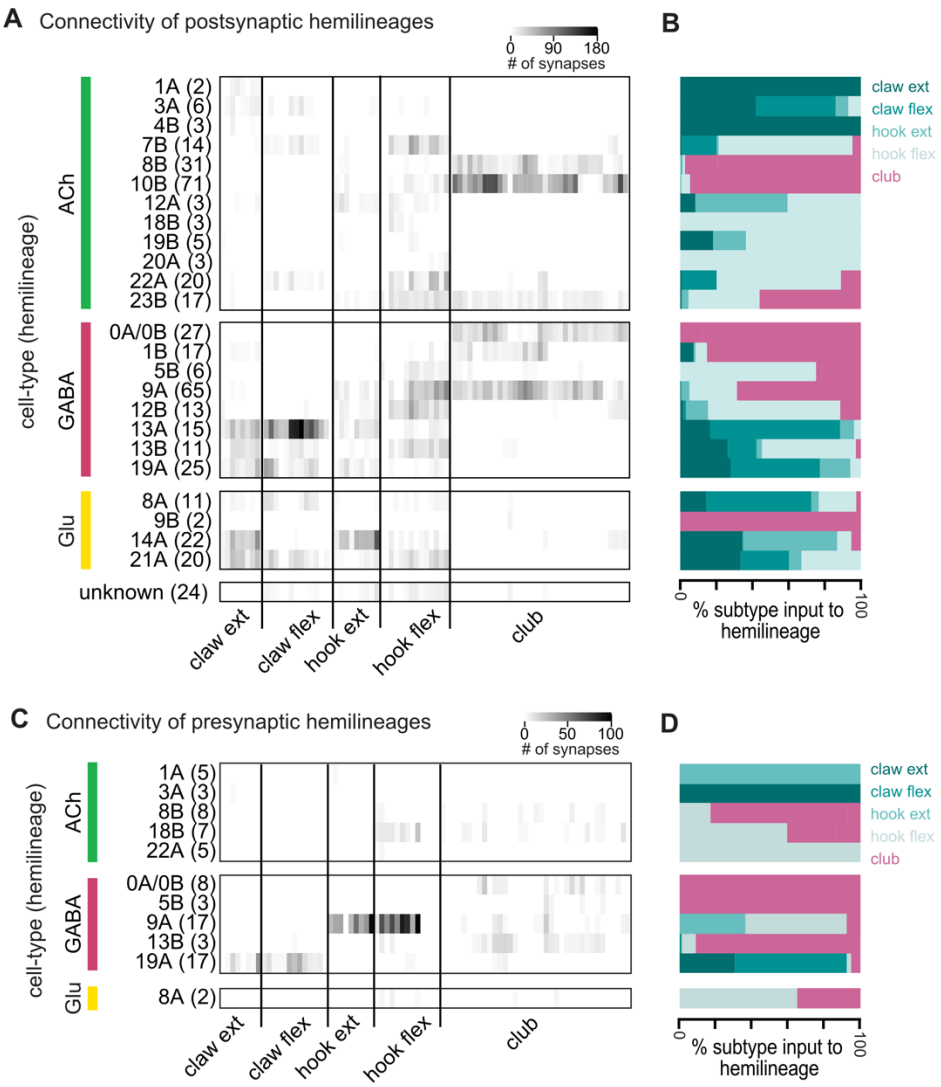

Figure S2.2 Subtypes of FeCO axons preferentially synapse with VNC neurons from specific developmental lineages. (A) The total number of synapses made by each FeCO neuron (columns) onto VNC neurons of each hemilineage (rows). Hemilineage was identified based on morphological characteristics of VNC neurons (see methods). Only local, ascending, and intersegmental postsynaptic partners are included in this analysis. VNC neurons of a given hemilineage are grouped together, with the number of neurons in each hemilineage indicated in parentheses. Hemilineages are grouped according to their primary neurotransmitter (ACh: acetylcholine, GABA: Gamma-aminobutyric acid, Glu: glutamate). (B) Percent of total FeCO input to a hemilineage made by each FeCO subtype. (C) The total number of synapses onto each FeCO neuron (columns) by presynaptic VNC neurons of each hemilineage (rows). (D) Percent of total inputs by a hemilineage onto each FeCO subtype.

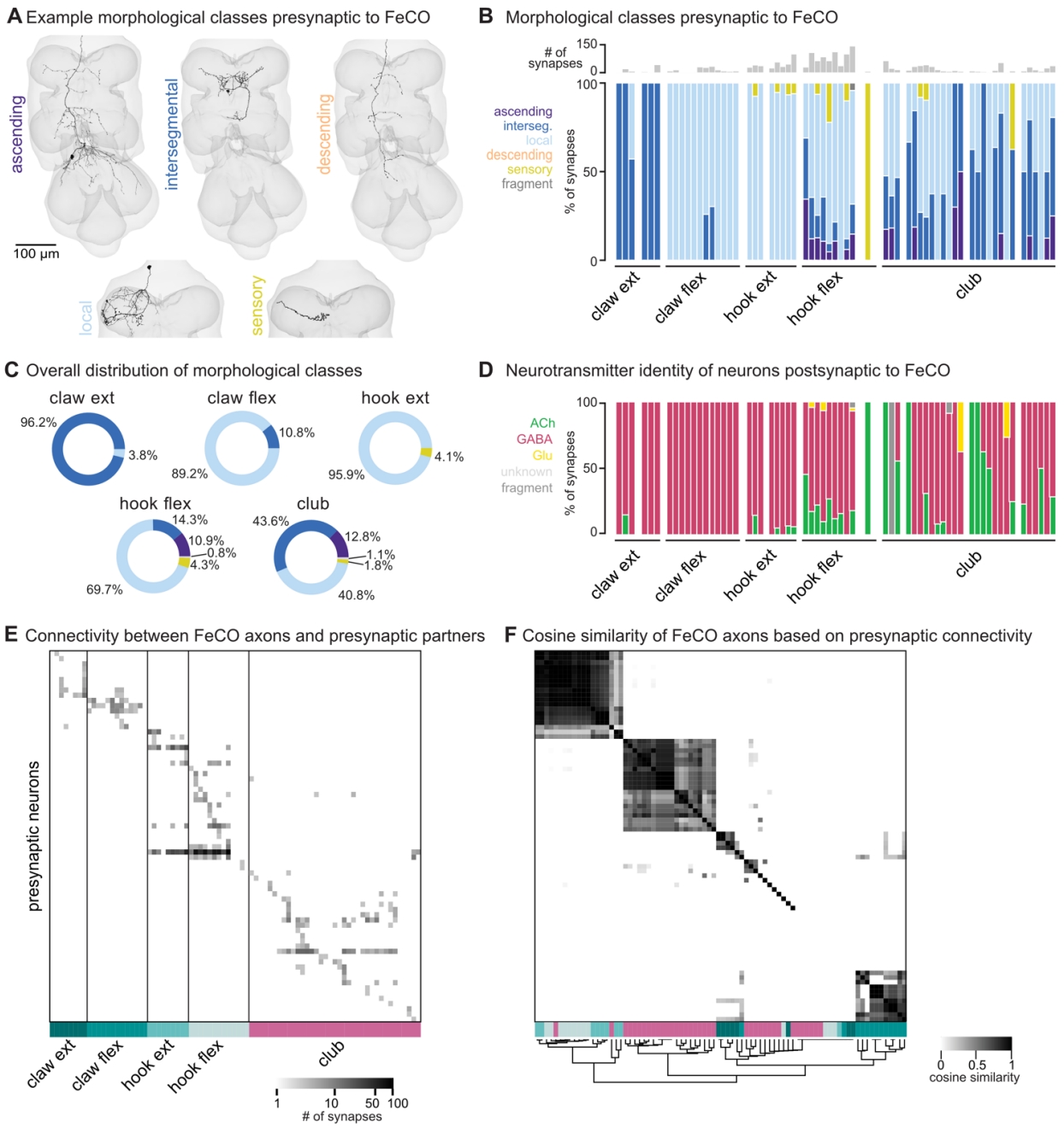

Figure S2.3 FeCO neurons exhibit subtype-specific presynaptic connectivity. (A) We reconstructed all VNC neurons presynaptic to FeCO axons from the front left leg (T1L) and classified them into morphological classes: ascending, descending, intersegmental, local, and sensory. Example provided from each class. (B) Percent of synapses received by each FeCO axon from VNC neurons of each morphological class. Top bar plot shows the total number of input synapses received by each FeCO axon. (C) Per FeCO subtype, the total fraction of input synapses received from each morphological class. (D) Proportion of total synapses made onto each FeCO neuron by presynaptic cholinergic (green), glutamatergic (yellow), GABAergic (pink), and unidentified (light gray) hemilineages. (E) Connectivity matrix between FeCO axons and presynaptic VNC neurons. The shading of each tick indicates the number of synapses from each presynaptic VNC neuron (row) onto each FeCO axon (column). Colored bars along the bottom indicate the postsynaptic FeCO subtype for that column. FeCO axons are organized by morphological subtype and then by their cosine similarity scores. VNC neurons are organized by their cosine similarity scores. (F) Clustered pairwise cosine similarity matrices of all FeCO axons based on their presynaptic connectivity. FeCO neurons with similar presynaptic connectivity patterns cluster together, forming connectivity clusters.

Supplemental Table 2.1 Neuroglancer links to FeCO axons by subtype

Club	https://neuromancer-seung-import.appspot.com/?json_url=https://raw.githubusercontent.com/sagrawal/Le e_2024/main/jsons/clubs.json
Hook extension	https://neuromancer-seung-import.appspot.com/?json_url=https://raw.githubusercontent.com/sagrawal/Le e_2024/main/jsons/hookE.json
Hook flexion	https://neuromancer-seung-import.appspot.com/?json_url=https://raw.githubusercontent.com/sagrawal/Le e_2024/main/jsons/hookF.json
Claw extension	https://neuromancer-seung-import.appspot.com/?json_url=https://raw.githubusercontent.com/sagrawal/Le e_2024/main/jsons/clawE.json
Claw flexion	https://neuromancer-seung-import.appspot.com/?json_url=https://raw.githubusercontent.com/sagrawal/Le e_2024/main/jsons/clawF.json

Supplemental Table 2.2 Neuroglancer links to VNC neurons by hemilineage

All presynaptic partners	https://neuromancer-seung-import.appspot.com/?json_url=https://raw.githubusercontent.com/sagrawal/Lee_2024/main/jsons/all_upstream.json
All postsynaptic partners	https://neuromancer-seung-import.appspot.com/?json_url=https://raw.githubusercontent.com/sagrawal/Lee_2024/main/jsons/all_downstream.json
Postsynaptic 0A/0B	https://neuromancer-seung-import.appspot.com/?json_url=https://raw.githubusercontent.com/sagrawal/Lee_2024/main/jsons/DS_0a0b.json
Postsynaptic 1A	https://neuromancer-seung-import.appspot.com/?json_url=https://raw.githubusercontent.com/sagrawal/Lee_2024/main/jsons/DS_1A.json
Postsynaptic 1B	https://neuromancer-seung-import.appspot.com/?json_url=https://raw.githubusercontent.com/sagrawal/Lee_2024/main/jsons/DS_1B.json
Postsynaptic 3A	https://neuromancer-seung-import.appspot.com/?json_url=https://raw.githubusercontent.com/sagrawal/Lee_2024/main/jsons/DS_3A.json

Postsynaptic 4B	https://neuromancer-seung-import.appspot.com/?json_url=https://raw.githubusercontent.com/sagrawal/Lee_2024/main/jsons/DS_4B.json
Postsynaptic 5B	https://neuromancer-seung-import.appspot.com/?json_url=https://raw.githubusercontent.com/sagrawal/Lee_2024/main/jsons/DS_5B.json
Postsynaptic 7B	https://neuromancer-seung-import.appspot.com/?json_url=https://raw.githubusercontent.com/sagrawal/Lee_2024/main/jsons/DS_7B.json
Postsynaptic 8A	https://neuromancer-seung-import.appspot.com/?json_url=https://raw.githubusercontent.com/sagrawal/Lee_2024/main/jsons/DS_8A.json
Postsynaptic 8B	https://neuromancer-seung-import.appspot.com/?json_url=https://raw.githubusercontent.com/sagrawal/Lee_2024/main/jsons/DS_8B.json
Postsynaptic 9A	https://neuromancer-seung-import.appspot.com/?json_url=https://raw.githubusercontent.com/sagrawal/Lee_2024/main/jsons/DS_9A.json
Postsynaptic 9B	https://neuromancer-seung-import.appspot.com/?json_url=https://raw.githubusercontent.com/sagrawal/L

	ee_2024/main/jsons/DS_9B.json
Postsynaptic 10B	https://neuromancer-seung-import.appspot.com/?json_url=https://raw.githubusercontent.com/sagrawal/Lee_2024/main/jsons/DS_10B.json
Postsynaptic 12A	https://neuromancer-seung-import.appspot.com/?json_url=https://raw.githubusercontent.com/sagrawal/Lee_2024/main/jsons/DS_12A.json
Postsynaptic 12B	https://neuromancer-seung-import.appspot.com/?json_url=https://raw.githubusercontent.com/sagrawal/Lee_2024/main/jsons/DS_12B.json
Postsynaptic 13A	https://neuromancer-seung-import.appspot.com/?json_url=https://raw.githubusercontent.com/sagrawal/Lee_2024/main/jsons/DS_13A.json
Postsynaptic 13B	https://neuromancer-seung-import.appspot.com/?json_url=https://raw.githubusercontent.com/sagrawal/Lee_2024/main/jsons/DS_13B.json
Postsynaptic 14A	https://neuromancer-seung-import.appspot.com/?json_url=https://raw.githubusercontent.com/sagrawal/Lee_2024/main/jsons/DS_14A.json
Postsynaptic	https://neuromancer-seung-

18B	import.appspot.com/?json_url=https://raw.githubusercontent.com/sagrawal/Lee_2024/main/jsons/DS_18B.json
Postsynaptic 19A	https://neuromancer-seung-import.appspot.com/?json_url=https://raw.githubusercontent.com/sagrawal/Lee_2024/main/jsons/DS_19A.json
Postsynaptic 19B	https://neuromancer-seung-import.appspot.com/?json_url=https://raw.githubusercontent.com/sagrawal/Lee_2024/main/jsons/DS_19B.json
Postsynaptic 20A	https://neuromancer-seung-import.appspot.com/?json_url=https://raw.githubusercontent.com/sagrawal/Lee_2024/main/jsons/DS_20A.json
Postsynaptic 21A	https://neuromancer-seung-import.appspot.com/?json_url=https://raw.githubusercontent.com/sagrawal/Lee_2024/main/jsons/DS_21A.json
Postsynaptic 22A	https://neuromancer-seung-import.appspot.com/?json_url=https://raw.githubusercontent.com/sagrawal/Lee_2024/main/jsons/DS_22A.json
Postsynaptic 23B	https://neuromancer-seung-import.appspot.com/?json_url=https://raw.githubusercontent.com/sagrawal/Lee_2024/main/jsons/DS_23B.json

Postsynaptic motor neurons	https://neuromancer-seung-import.appspot.com/?json_url=https://raw.githubusercontent.com/sagrawal/Lee_2024/main/jsons/MN.json
Postsynaptic unknown	https://neuromancer-seung-import.appspot.com/?json_url=https://raw.githubusercontent.com/sagrawal/Lee_2024/main/jsons/unknown.json

Supplemental Table 2.3 Neuroglancer links to ascending club, 8B, and 10B neurons in Flywire

Ascending neurons	ascending club neurons ascending 8B/10B neurons

References

1. Lee, S.-Y. J., Dallmann, C. J., Cook, A., Tuthill, J. C. & Agrawal, S. Divergent neural circuits for proprioceptive and exteroceptive sensing of the Drosophila leg. 2024.04.23.590808 Preprint at https://doi.org/10.1101/2024.04.23.590808 (2024).
2. O'Connor, D. H., Krubitzer, L. & Bensmaia, S. Of mice and monkeys: Somatosensory processing in two prominent animal models. *Prog. Neurobiol.* **201**, 102008 (2021).
3. Tuthill, J. C. & Wilson, R. I. Mechanosensation and Adaptive Motor Control in Insects. *Curr. Biol.* **26**, R1022–R1038 (2016).
4. Turecek, J. & Ginty, D. D. Coding of self and environment by Pacinian neurons in freely moving animals. 2023.09.11.557225 Preprint at https://doi.org/10.1101/2023.09.11.557225 (2023).
5. Reschechtko, S. & Pruszynski, J. A. Stretch reflexes. *Curr. Biol. CB* **30**, R1025–R1030 (2020).
6. Abraira, V. E. & Ginty, D. D. The Sensory Neurons of Touch. *Neuron* **79**, 618–639 (2013).
7. Macefield, V. G. The roles of mechanoreceptors in muscle and skin in human proprioception. *Curr. Opin. Physiol.* **21**, 48–56 (2021).
8. Dorkenwald, S. *et al.* Neuronal wiring diagram of an adult brain. *bioRxiv* 2023.06.27.546656 (2023) doi:10.1101/2023.06.27.546656.
9. Phelps, J. S. *et al.* Reconstruction of motor control circuits in adult *Drosophila* using automated transmission electron microscopy. *Cell* **184**, 759-774.e18 (2021).
10. Takemura, S. *et al.* A Connectome of the Male Drosophila Ventral Nerve Cord. 2023.06.05.543757 Preprint at https://doi.org/10.1101/2023.06.05.543757 (2023).
11. Winding, M. *et al.* The connectome of an insect brain. *Science* **379**, eadd9330 (2023).

12. Zheng, Z. *et al.* A Complete Electron Microscopy Volume of the Brain of Adult *Drosophila melanogaster*. *Cell* **174**, 730-743.e22 (2018).

13. Hampel, S. *et al.* Distinct subpopulations of mechanosensory chordotonal organ neurons elicit grooming of the fruit fly antennae. *eLife* **9**, e59976 (2020).

14. Kim, H. *et al.* Wiring patterns from auditory sensory neurons to the escape and song-relay pathways in fruit flies. *J. Comp. Neurol.* **528**, 2068–2098 (2020).

16. Mamiya, A., Gurung, P. & Tuthill, J. C. Neural coding of leg proprioception in Drosophila. *Neuron* **100**, 636–650 (2018).

17. Phillis, R., Statton, D., Caruccio, P. & Murphey, R. K. Mutations in the 8 kDa dynein light chain gene disrupt sensory axon projections in the Drosophila imaginal CNS. *Development* **122**, 2955–2963 (1996).

18. Smith, S. A. & Shepherd, D. Central afferent projections of proprioceptive sensory neurons in Drosophila revealed with the enhancer-trap technique. *J. Comp. Neurol.* **364**, 311–323 (1996).

19. Field, L. H. & Matheson, T. Chordotonal Organs of Insects. in *Advances in Insect Physiology* (ed. Evans, P. D.) vol. 27 1–228 (Academic Press, 1998).

20. Mamiya, A. *et al.* Biomechanical origins of proprioceptor feature selectivity and topographic maps in the *Drosophila* leg. *Neuron* **111**, 3230-3243.e14 (2023).

21. Eberhard, M. J. B. *et al.* Structure and sensory physiology of the leg scolopidial organs in Mantophasmatodea and their role in vibrational communication. *Arthropod Struct. Dev.* **39**, 230–241 (2010).

22. Field, L. H. & Pflüger, H.-J. The femoral chordotonal organ: A bifunctional orthopteran (Locusta migratoria) sense organ? *Comp. Biochem. Physiol. A Physiol.* **93**, 729–743 (1989).

23. McKelvey, E. G. Z. *et al.* Drosophila females receive male substrate-borne signals through specific leg neurons during courtship. *Curr. Biol.* **31**, 3894-3904.e5 (2021).

24. Takanashi, T., Fukaya, M., Nakamuta, K., Skals, N. & Nishino, H. Substrate vibrations mediate behavioral responses via femoral chordotonal organs in a cerambycid beetle. *Zool. Lett.* **2**, 18 (2016).

25. Agrawal, S. *et al.* Central processing of leg proprioception in *Drosophila*. *eLife* **9**, e60299 (2020).

26. Chen, C. *et al.* Functional architecture of neural circuits for leg proprioception in *Drosophila*. *Curr Biol* **31**, 5163-5175.e7 (2021).

27. Azevedo, A. *et al.* Tools for comprehensive reconstruction and analysis of *Drosophila* motor circuits. (2022) doi:10.1101/2022.12.15.520299.

28. Lesser, E. *et al.* Synaptic architecture of leg and wing motor control networks in *Drosophila*. *bioRxiv* 2023.05.30.542725 (2023) doi:10.1101/2023.05.30.542725.

29. Azevedo, A. W. *et al.* A size principle for recruitment of Drosophila leg motor neurons. *Elife* **9**, e56754 (2020).

30. Dallmann, C. J., Agrawal, S., Cook, A., Brunton, B. W. & Tuthill, J. C. Presynaptic inhibition selectively suppresses leg proprioception in behaving *Drosophila*. *bioRxiv* 2023.10.20.563322 (2023).

31. Scheffer, L. K. *et al.* A connectome and analysis of the adult Drosophila central brain. *eLife* **9**, e57443 (2020).

32. Schlegel, P. *et al.* Whole-brain annotation and multi-connectome cell typing quantifies circuit stereotypy in Drosophila. 2023.06.27.546055 Preprint at https://doi.org/10.1101/2023.06.27.546055 (2023).

33. Truman, J. W., Moats, W., Altman, J., Marin, E. C. & Williams, D. W. Role of Notch signaling in establishing the hemilineages of secondary neurons in Drosophila melanogaster. *Development* **137**, 53–61 (2010).

34. Lacin, H. *et al.* Neurotransmitter identity is acquired in a lineage-restricted manner in the *Drosophila* CNS. *eLife* **8**, e43701 (2019).

35. Allen, A. M. *et al.* A single-cell transcriptomic atlas of the adult Drosophila ventral nerve cord. *bioRxiv* 2019.12.20.883884 (2019) doi:10.1101/2019.12.20.883884.

36. Lacin, H. & Truman, J. W. Lineage mapping identifies molecular and architectural similarities between the larval and adult Drosophila central nervous system. *eLife* **5**, e13399 (2016).

37. Harris, R. M., Pfeiffer, B. D., Rubin, G. M. & Truman, J. W. Neuron hemilineages provide the functional ground plan for the *Drosophila* ventral nervous system. *eLife* **4**, e04493 (2015).

38. Mark, B. *et al.* A developmental framework linking neurogenesis and circuit formation in the Drosophila CNS. *eLife* **10**, e67510 (2021).

39. Li, H. *et al.* Fly Cell Atlas: A single-nucleus transcriptomic atlas of the adult fruit fly. *Science* **375**, eabk2432 (2022).

40. Gowda, S. B. M. *et al.* GABAergic inhibition of leg motoneurons is required for normal walking behavior in freely moving Drosophila. *Proc. Natl. Acad. Sci.* **115**, E2115–E2124 (2018).

41. Lees, K. *et al.* Actions of agonists, fipronil and ivermectin on the predominant in vivo splice and edit variant (RDLbd, I/V) of the Drosophila GABA receptor expressed in Xenopus laevis oocytes. *PloS One* **9**, e97468 (2014).

42. Liu, W. W. & Wilson, R. I. Glutamate is an inhibitory neurotransmitter in the Drosophila olfactory system. *Proc. Natl. Acad. Sci. U. S. A.* **110**, 10294–10299 (2013).

43. Zill, S. N., Chaudhry, S., Büschges, A. & Schmitz, J. Force feedback reinforces muscle synergies in insect legs. *Arthropod Struct. Dev.* **44**, 541–553 (2015).

44. King, D. G. & Wyman, R. J. Anatomy of the giant fibre pathway in Drosophila. I. Three thoracic components of the pathway. *J. Neurocytol.* **9**, 753–770 (1980).

45. Tanouye, M. A. & Wyman, R. J. Motor outputs of giant nerve fiber in Drosophila. *J. Neurophysiol.* **44**, 405–421 (1980).

46. Patella, P. & Wilson, R. I. Functional Maps of Mechanosensory Features in the Drosophila Brain. *Curr. Biol. CB* **28**, 1189-1203.e5 (2018).

47. Ishikawa, Y., Okamoto, N., Nakamura, M., Kim, H. & Kamikouchi, A. Anatomic and Physiologic Heterogeneity of Subgroup-A Auditory Sensory Neurons in Fruit Flies. *Front. Neural Circuits* **11**, 46 (2017).

48. Yorozu, S. *et al.* Distinct sensory representations of wind and near-field sound in the Drosophila brain. *Nature* **458**, 201–205 (2009).

49. Matsuo, E. *et al.* Organization of projection neurons and local neurons of the primary auditory center in the fruit fly Drosophila melanogaster. *J. Comp. Neurol.* **524**, 1099–1164 (2016).

50. Baker, C. A. *et al.* Neural network organization for courtship-song feature detection in Drosophila. *Curr. Biol. CB* **32**, 3317-3333.e7 (2022).

51. Burrows, M. & Horridge, G. A. The organization of inputs to motoneurons of the locust metathoracic leg. *Philos. Trans. R. Soc. Lond. B. Biol. Sci.* **269**, 49–94 (1974).

52. Field, L. H. & Rind, F. C. A single insect chordotonal organ mediates inter- and intra-segmental leg reflexes. *Comp. Biochem. Physiol. A Physiol.* **68**, 99–102 (1981).

53. Azim, E. & Seki, K. Gain control in the sensorimotor system. *Curr. Opin. Physiol.* **8**, 177–187 (2019).

54. Koch, S. C. *et al.* RORβ Spinal Interneurons Gate Sensory Transmission during Locomotion to Secure a Fluid Walking Gait. *Neuron* **96**, 1419-1431.e5 (2017).

55. McComas, A. J. Hypothesis: Hughlings Jackson and presynaptic inhibition: is there a big picture? *J. Neurophysiol.* **116**, 41–50 (2016).

56. Chockley, A. S. *et al.* Subsets of leg proprioceptors influence leg kinematics but not interleg coordination in Drosophila melanogaster walking. *J. Exp. Biol.* **225**, jeb244245 (2022).

57. Delcomyn, F. Factors Regulating Insect Walking. *Annu. Rev. Entomol.* **30**, 239–256 (1985).

58. Pratt, B. G., Lee, S.-Y. J., Chou, G. M. & Tuthill, J. C. Miniature linear and split-belt treadmills reveal mechanisms of adaptive motor control in walking Drosophila. 2024.02.23.581656 Preprint at https://doi.org/10.1101/2024.02.23.581656 (2024).

59. Laurent, G. & Burrows, M. Intersegmental interneurons can control the gain of reflexes in adjacent segments of the locust by their action on nonspiking local interneurons. *J. Neurosci. Off. J. Soc. Neurosci.* **9**, 3030–3039 (1989).

60. Chen, C.-L. *et al.* Ascending neurons convey behavioral state to integrative sensory and action selection brain regions. *Nat. Neurosci.* **26**, 682–695 (2023).

61. Cruz, T. L. & Chiappe, M. E. Multilevel visuomotor control of locomotion in *Drosophila*. *Curr. Opin. Neurobiol.* **82**, 102774 (2023).

62. Fujiwara, T., Brotas, M. & Chiappe, M. E. Walking strides direct rapid and flexible recruitment of visual circuits for course control in *Drosophila*. *Neuron* **110**, 2124-2138.e8 (2022).

63. Pfeiffer, K. & Homberg, U. Organization and functional roles of the central complex in the insect brain. *Annu. Rev. Entomol.* **59**, 165–184 (2014).

65. Hill, P. S. M. & Wessel, A. Biotremology. *Curr. Biol.* **26**, R187–R191 (2016).

66. Huey, E. L. *et al.* The auditory midbrain mediates tactile vibration sensing. *bioRxiv* 2024.03.08.584077 (2024) doi:10.1101/2024.03.08.584077.

67. Virant-Doberlet, M., Stritih-Peljhan, N., Žunič-Kosi, A. & Polajnar, J. Functional Diversity of Vibrational Signaling Systems in Insects. *Annu. Rev. Entomol.* **68**, 191–210 (2023).

68. Burke, W. An Organ for Proprioception and Vibration Sense in Carcinus Maenas. *J. Exp. Biol.* **31**, 127–138 (1954).

69. Cohen, M. J. The crustacean myochordotonal organ as a proprioceptive system. *Comp. Biochem. Physiol.* **8**, 223–243 (1963).

70. Salmon, M., Horch, K. & Hyatt, G. Barth's myochordotonal organ as a receptor for auditory and vibrational stimuli in fiddler crabs (Uca pugilator and U. minax). *Mar. Freshw. Behav. Phy* **4**, 187–194 (1977).

71. Ewing, A. W. & Bennet-Clark, H. C. The Courtship Songs of Drosophila. *Behaviour* **31**, 288–301 (1968).

72. Kamikouchi, A. *et al.* The neural basis of Drosophila gravity-sensing and hearing. *Nature* **458**, 165–171 (2009).

73. Murthy, M. Unraveling the auditory system of *Drosophila*. *Curr. Opin. Neurobiol.* **20**, 281–287 (2010).

74. Shorey, H. H. Nature of the Sound Produced by Drosophila melanogaster during Courtship. *Science* **137**, 677–678 (1962).

75. Fabre, C. C. G. *et al.* Substrate-Borne Vibratory Communication during Courtship in Drosophila melanogaster. *Curr. Biol.* **22**, 2180–2185 (2012).

76. Gebehart, C., Hooper, S. L. & Büschges, A. Non-linear multimodal integration in a distributed premotor network controls proprioceptive reflex gain in the insect leg. *Curr. Biol. CB* **32**, 3847-3854.e3 (2022).

77. Gebehart, C. & Büschges, A. The processing of proprioceptive signals in distributed networks: insights from insect motor control. *J. Exp. Biol.* **227**, jeb246182 (2024).

78. Maitin-Shepard, J. *et al.* google/neuroglancer: Zenodo https://doi.org/10.5281/zenodo.5573294 (2021).

79. Dorkenwald, S. *et al.* CAVE: Connectome Annotation Versioning Engine. *bioRxiv* 2023.07.26.550598 (2023) doi:10.1101/2023.07.26.550598.

80. Marin, E. C. *et al.* Systematic annotation of a complete adult male *Drosophila* nerve cord connectome reveals principles of functional organisation. *bioRxiv* 2023.06.05.543407 (2023) doi:10.1101/2023.06.05.543407.

81. Meissner, G. W. *et al.* A searchable image resource of *Drosophila* GAL4 driver expression patterns with single neuron resolution. *eLife* **12**, e80660 (2023).

82. Buhmann, J. *et al.* Automatic detection of synaptic partners in a whole-brain Drosophila electron microscopy data set. *Nat. Methods* **18**, 771–774 (2021).

83. Dorkenwald, S. *et al.* FlyWire: online community for whole-brain connectomics. *Nat. Methods* **19**, 119–128 (2022).

84. Matsliah, A. *et al.* Neuronal "parts list" and wiring diagram for a visual system. *bioRxiv* 2023.10.12.562119 (2023) doi:10.1101/2023.10.12.562119.

85. Eckstein, N. *et al.* Neurotransmitter Classification from Electron Microscopy Images at Synaptic Sites in Drosophila Melanogaster. 2020.06.12.148775 Preprint at https://doi.org/10.1101/2020.06.12.148775 (2023).

86. Heinrich, L., Funke, J., Pape, C., Nunez-Iglesias, J. & Saalfeld, S. Synaptic Cleft Segmentation in Non-isotropic Volume Electron Microscopy of the Complete Drosophila Brain. in *Medical Image Computing and Computer Assisted Intervention – MICCAI 2018* (eds. Frangi, A. F., Schnabel, J. A., Davatzikos, C., Alberola-López, C. & Fichtinger, G.) 317–325 (Springer International Publishing, Cham, 2018). doi:10.1007/978-3-030-00934-2_36.

Chapter 3

CHARACTERIZING NEUROPEPTIDE MODULATION OF SENSORIMOTOR CIRCUITS AND BEHAVIOR IN *DROSOPHILA*

Su-Yee J. Lee, John C. Tuthill

3.0.1 Note:

This Chapter is a work in progress.

3.1 Abstract

Motor behavior dynamically shifts depending on the internal state of the organism. Chemical messengers, such as neuromodulatory amines and peptides, are released in a state-dependent manner and flexibly modulate sensorimotor circuit activity in accordance with the state of the organism. While much is known about the physiological effects of neuromodulators on sensorimotor circuits in *ex vivo* preparations, the role that neuromodulators play in *in vivo* circuits and behavior remains unclear. In this work, we used the genetic and experimental toolkit in *Drosophila* to investigate how neuromodulatory systems alter sensorimotor circuits and behavior in intact systems. First, we conducted a behavior screen, quantifying how activation of

neuromodulatory systems in *Drosophila* alter walking behaviors. We found that activation of Allatostatin A (AstA) and Myosuppressin (Ms) releasing neurons causes flies to rapidly stop movement or start running, respectively. Using confocal imaging, RNA-seq, and calcium imaging, we further investigated the modulatory effects of AstA and Ms on sensorimotor circuits in the ventral nerve cord. Altogether, this project may serve as a technical roadmap for future investigations of neuromodulation of sensorimotor circuits in *Drosophila*.

3.2 Introduction

Animal movement is adaptive: responsive to changes in both the environment and the organism's internal needs. Neuromodulators, chemical messengers that bind to G-protein coupled receptors, are important for altering sensorimotor circuit activity in a state-dependent manner to support adaptive motor output. For example, octopamine, the insect homolog of noradrenaline, is released into the hemolymph after high-energy activity and acts on multiple systems in the body to "orchestrate" the transition to flight[1,2]. Octopamine induces a consortium of flight-related changes to neural activity, including: promoting bursting in locust flight interneurons[3] and increasing activity in *Drosophila* visual neurons to enhance visual motion processing[4,5]. Octopamine is one of many chemical messengers with well-documented modulatory effects on motor behavior and sensorimotor circuits[6–10]. While these studies highlight the role that neuromodulators play in driving and regulating sensorimotor circuits, the direct mechanisms linking the changes in neural activity to behavior are less clear.

Decades of research on the stomatogastric ganglion (STG), a central pattern generator that controls digestive and chewing behaviors in crustaceans, provides the most detailed information

on the physiological effects of neuromodulators on a sensorimotor circuit[8,11]. This body of work gives insight into the vast number of operations that neuromodulators can perform on a small, 30 neuron circuit. Neuromodulators have widespread and powerful effects, from altering intrinsic firing properties of single neurons to switching entire circuit modes[12]. The recordings in the STG circuit are typically performed in dissected preparations using single cell electrophysiology, however. As a result, it is unclear how the principles learned from *ex vivo* preparations apply to *in vivo* circuits and behavior.

To understand how neuromodulators contribute to adaptive movement, it is critical to probe sensorimotor circuits in awake, behaving animals. Progressive technological advances in genetics[13–15], neural recording[16], and neural manipulation[17,18], now enable investigations into neuromodulation of neural circuits and behavior in intact systems. In *Drosophila,* these tools have particularly advanced our understanding of the neural circuits and neuromodulators that regulate sleep-wake cycles[19–24] and circadian rhythms[25–27]. These studies are centrally focused on the brain, however, and overlook the influence of neuromodulators on sensorimotor circuits in the ventral nerve cord (VNC) and peripheral nervous system.

Sleep-wake cycles and circadian rhythms are high-level, complex internal states that are commonly measured through changes in overall motor activity[28] or responses to arousing sensory stimuli[29]. Thus, it is imperative to study how sensorimotor circuits in the VNC are affected by changes in global states. For example, Donlea et al (2011) discovered a sleep-switch neuron in the central complex of the brain that rapidly induces sleep when activated[23]. Several follow-up studies dissected the neural circuits and neuromodulators, particularly the neuropeptide Allatostatin A (AstA), that regulate the sleep-switch circuit in the brain[22,30–32]. Recent evidence, however, identified local VNC neurons within the AstA receptor genetic driver line used to target the sleep-

switch neurons that are capable of recapitulating sleep-like behaviors[33]. This finding suggests that neurons local to the VNC could act in parallel to the sleep-switch neurons in the brain or promote changes to movement unrelated to sleep, such as paralysis. This example highlights the importance of investigating modulation of sensorimotor circuits central to the VNC, especially when using motor behavior assays to quantify changes in state.

What are the neural mechanisms for state-dependent modulation of sensorimotor circuits? The activity could be feedforward: internal state is centrally driven and regulated by neural mechanisms in the brain and appropriate motor commands are transmitted to the VNC. Alternatively, separate circuits in the VNC could act in parallel or independently of the brain to regulate internal state and support adaptive, state-dependent movement. Neuromodulators could serve as an important link between the brain and VNC, as they are released in a state-dependent manner and diffuse across the entire body to coordinate activity across multiple systems.

As a step towards understanding how neuromodulators alter sensorimotor circuits and behavior, we used the genetic and experimental toolkit of *Drosophila melanogaster* to dissect the neuromodulatory mechanisms central to the ventral nerve cord and peripheral nervous systems. First, we conducted an optogenetic activation screen, quantifying how activation of the major neuromodulatory systems in *Drosophila* alter motor behaviors. From this screen, we identified multiple neuromodulatory systems that significantly and robustly alter locomotion. We focused specifically on two neuropeptide systems, Allatostatin A (AstA) and Myosuppressin (Ms), which cause flies to cease movement or start running after optogenetic activation, respectively. This finding suggests that AstA and Ms release could induce drastic global state or behavior switches, from movement to inactivity or vice versa. We found that AstA and Ms receptors are expressed in the femoral chordotonal organ (FeCO) in the leg, somatosensory stretch receptors that detect

movement, position, and vibration of the leg[34,35] and are involved in behaviors such as walking, postural control, and social communication[36–39]. We further quantified the physiological effects of AstA and Ms on FeCO neurons and recorded calcium activity from the axons in the VNC while bath applying neuropeptides. Altogether, we hypothesize that AstA and Ms suppress FeCO sensing to dampen sensory thresholds during states such as rest or high-speed locomotion. Overall, the results from these experiments were inconclusive but here we report the methods, results, and conclusions.

3.3 Results

Neuromodulators alter walking behavior in fruit flies

Neuromodulators target all parts of the sensorimotor circuit, including muscles, sensory neurons, interneurons, and motor neurons[40]. Neuromodulators could act on a high-level, providing the switch to transition between behavior modes (e.g. rest to escape) or on a low-level, transiently targeting specific neurons to induce sudden, discrete behaviors such as kicking. To better understand which aspects of the sensorimotor circuit neuromodulators target, we conducted an optogenetic activation screen of neuromodulatory populations in *Drosophila* while tracking the statistics of walking in groups of freely moving flies. We screened through 31 Gal4 lines that genetically target neurons that release neuromodulatory peptides and amines in *Drosophila*. From this screen, we identified several candidate neuromodulatory systems that significantly alter locomotion after optogenetic activation (**Figure 3.1A**). Interestingly, we found that activation of neuromodulatory systems induce a diverse range of responses, including decreasing velocity (e.g. AstA, Ok, CCHa2, TrH, NPF, ITP, and ETH) and increasing velocity (e.g. HDC, CCHa1, Lk, Ms).

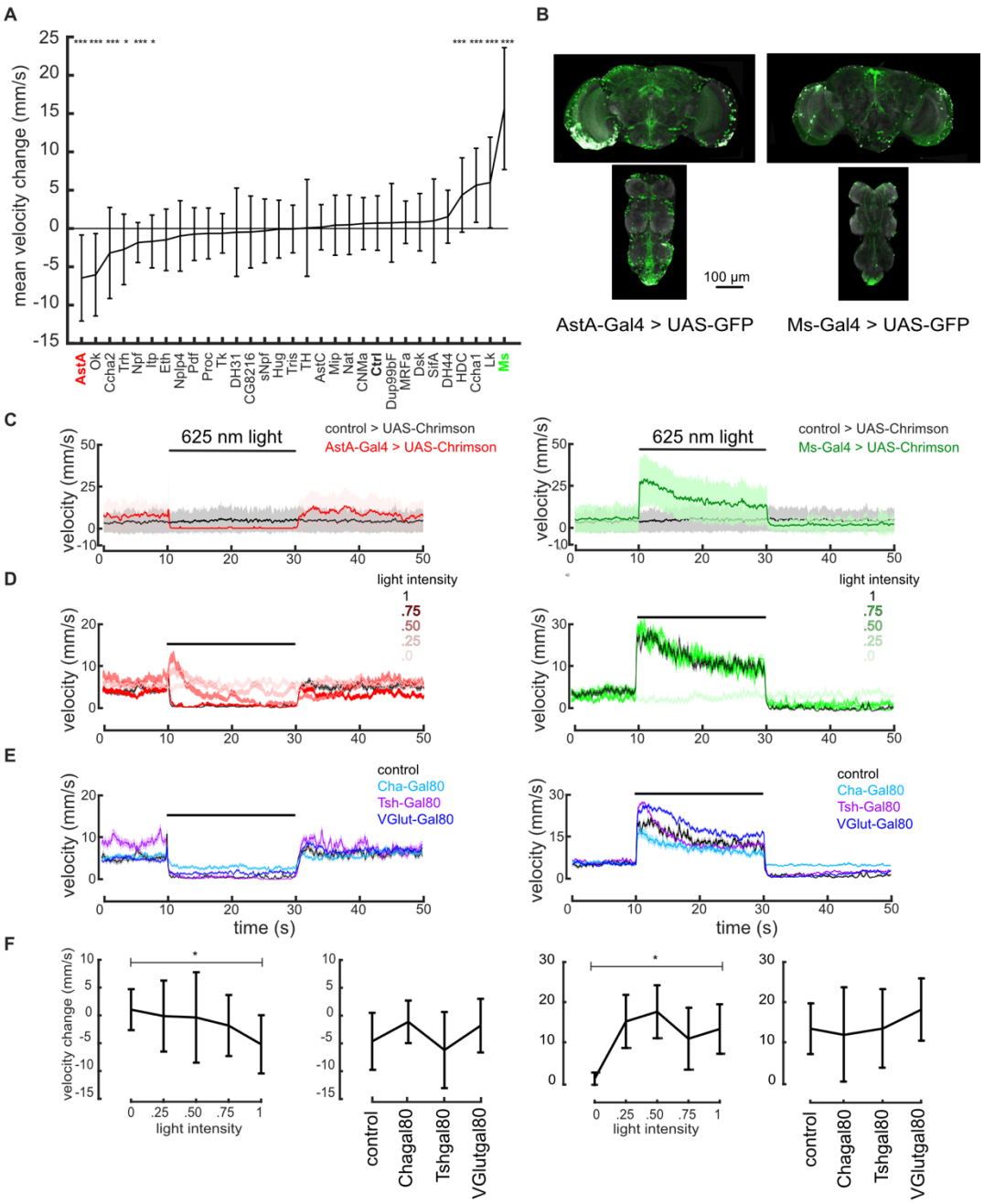

Figure 3.1 Optogenetic activation screen of neuromodulatory neurons. (A) Results from an optogenetic activation screen of 31 Gal4 lines targeting neuromodulatory neurons in *Drosophila.* Mean change in velocity ± standard deviation (std) of the population after optogenetic activation. Statistical significance indicated by *p < 0.05 *** p< 0.001, assessed using Mann-Whitney U test. (B) Confocal images showing expression of (left) AstA and (right) Ms releasing neurons in the brain and ventral nerve cord. Green, GFP driven by each Gal4 line; gray, nc82 neuropil staining. (C) Average velocity traces after red-light activation in AstA-Gal4>UAS-CsChrimson flies (red) or control flies (black), and Ms-Gal4>UAS-CsChrimson flies (green) or control flies (black). Shaded region indicates ± std. n = 27 for AstA, n = 46 for Ms. n = 57 for control. Split-half-Gal4>UAS-CsChrimson used as control. (D) Average velocity traces after red-light activation of AstA-Gal4>UAS-CsChrimson (left, red) and Ms-Gal4>UAS-CsChrimson (right, green) at different stimulus light intensities (1, 0.75, 0.50, 0.25, 0). Shaded region indicates ± standard error of the mean (SEM). N = 93, 97, 75, 99, 94 for AstA and N = 47, 50, 50, 50, 53 for Ms. (E) Velocity time-series of activation of AstA neurons (left) or Ms neurons (right) with either UAS-CsChrimson;Tsh-Gal80 (purple), Cha-Gal80 (light blue), or VGlut-Gal80 (dark blue) suppression. AstA N = 49, 34, 46. Ms N = 38, 44, 28. (F) Summary plots for D,E quantifying the mean change in velocity after optogenetic activation of each group. * p <0.05, Mann-Whitney U test. For all plots, the mean change in velocity is quantified by subtracting the mean velocity during a 10s baseline period preceding the stimulus from the mean velocity during the 10s stimulus period.

At the two extremes, we found that activation of neurons that release Allatostatin A (AstA) causes flies to cease movement for the duration of the stimulus, while activation of neurons that release Myosuppressin (Ms) induces high-speed running (average velocity ~30mm/s) (**Figure 3. 1B,C**). We further investigated the AstA and Ms systems in *Drosophila* due to their significant and robust effects on behavior.

Neurotransmitters and neuromodulators are released under different conditions. Low frequency stimulation is sufficient for reliably inducing synaptic vesicle exocytosis but not dense core vesicle release, which may require high frequency stimulation[41,42]. The parameters for inducing dense core vesicle release are not straightforward and likely vary depending on the type of neuron, chemical messenger, and state of the animal[43,44]. To improve the likelihood of activating dense core vesicle release, we designed a high-intensity and long-duration optogenetic activation stimulation protocol (4 mW/mm^2, 20s). We expect that low intensity protocols would be sufficient to induce synaptic transmission while high intensity protocols could activate neuromodulatory mechanisms, resulting in differential behavioral outcomes. To investigate whether the behavioral results were an outcome of neurotransmitter or neuromodulator action, we performed additional optogenetic activation experiments with AstA and Ms releasing neurons while varying the light intensity. After activation AstA and Ms releasing neurons under different light intensities there is no significant difference in the change in velocity (**Figure 3.1D, F**). This suggests that activation of the population of AstA or Ms releasing neurons induces a robust, uniform behavioral response.

Neurons are capable of releasing multiple chemical messengers, including a primary neurotransmitter and one or multiple neuromodulators[41,45]. As a consequence of these co-release properties, optogenetic activation of a genetically targeted neuron likely drives release of multiple chemical messengers. To specifically target neuromodulator release, we crossed the UAS-

CsChrimson line with Gal80 suppressors to restrict expression of genetically targeted populations within the Gal4 line. For example, using the Cha-Gal80 suppressor with AstA-Gal4>UAS-CsChrimson, we could exclude expression of cholinergic neurons within the Gal4 line. In addition to Cha-Gal80, we also used VGlut-Gal80 to exclude glutamatergic neurons, and tsh-Gal80 to exclude neurons in the VNC (although the line is not fully restrictive to the brain). After activation of AstA or Ms releasing neurons with restricted Gal80 expression, we observed no significant changes to the behavioral responses in these lines in any condition (**Figure 3.1E,F)**. In the context of tsh-Gal80, we found that although the Gal80 driver restricts expression it does not fully exclude expression in the VNC. Altogether, these findings show that the neurons driving the observed behavioral responses are not co-transmitted with acetylcholine or glutamate.

Expression of AstA and Ms receptors in FeCO neurons in the leg

Based on the behavior results and expression of AstA and Ms neurons in the VNC, we hypothesized that these neuropeptides modulate the sensorimotor circuits that control walking. Next, we looked at the expression of AstA and Ms receptors within the VNC and peripheral nervous system to characterize which sensorimotor circuits these neuropeptide target. We looked at the expression of two AstA receptors (AstAR1 and AstAR2) and one Ms receptor (MsR1) in the central nervous system (brain and VNC) and in the leg periphery. While we observed broad expression of AstAR1 and MsR1 in the central nervous system, we notably see expression of AstAR1 and MsR1 in the leg sensory neurons (**Figure 3.2A**). In contrast, we see little to no expression of AstAR2 in the central nervous system or leg sensory neurons.

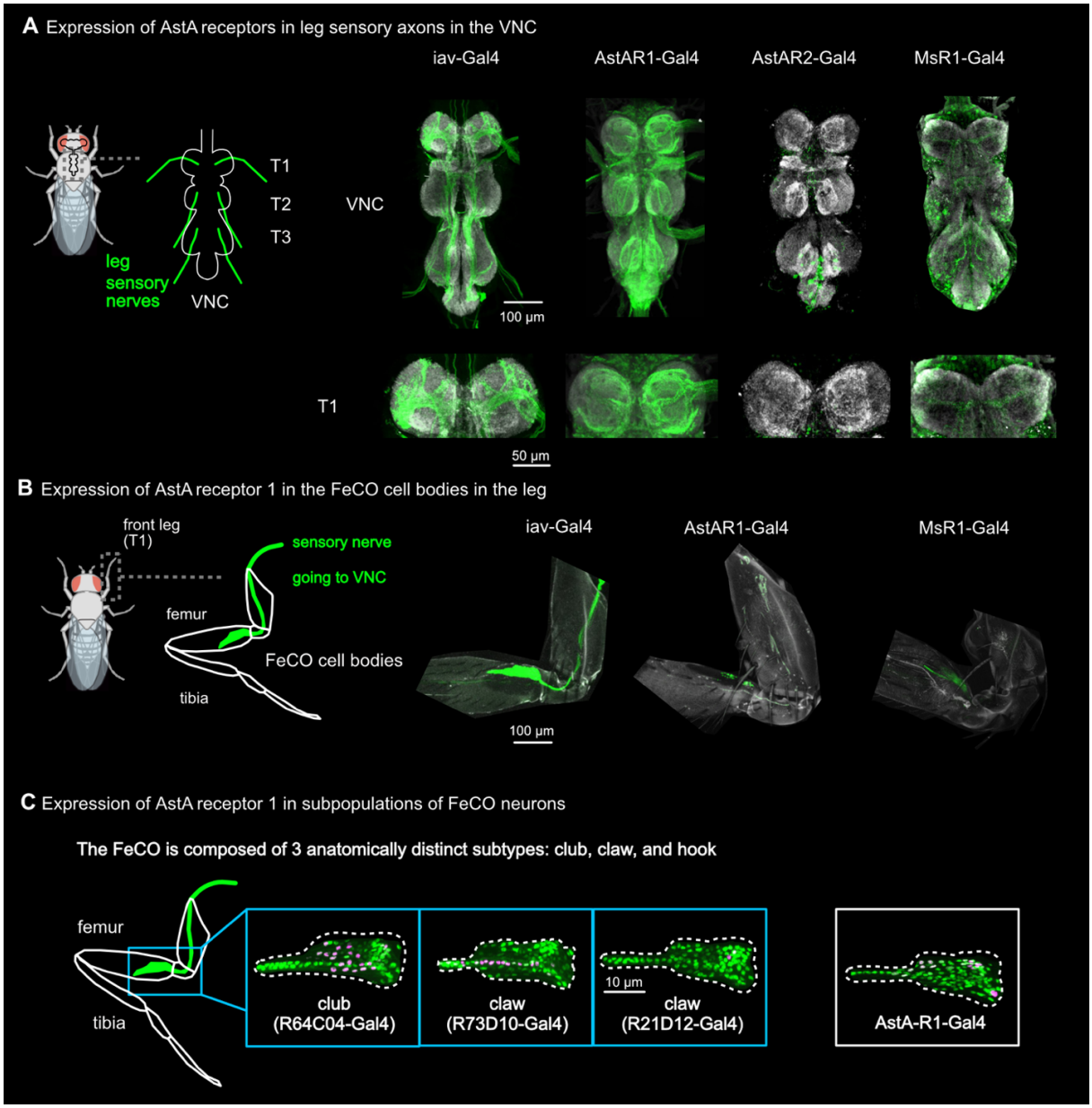

Figure 3.2 Expression of AstA and Ms receptors in the ventral nerve cord and periphery. (A) Left, schematic of leg sensory nerves projecting into the VNC in *Drosophila.* Right, confocal images of the VNC and T1 neuropils, which correspond to the front legs. From left to right: expression of FeCO axons, AstAR1, AstAR2, and MsR1 neurons in the VNC and T1 neuropils. Green, GFP driven by each Gal4 line; gray, nc82 neuropil staining. (B) Left, schematic of FeCO cell bodies in the femur of the front leg of *Drosophila* and the sensory axon which projects to the VNC. Right, confocal images of the coxa-femur joint of the front leg of *Drosophila*. Left to right: expression of FeCO cell bodies in the leg, expression of AstAR1 and MsR1 neurons in the FeCO. Green, GFP driven by each Gal4 line; gray, autofluorescence from the cuticle. (C) Left, schematic of the 3 cell types within the FeCO: club, claw, and hook. Confocal images of FeCO cell bodies in the front leg with each subtype labeled by each respective Gal4 line. Right, expression of AstAR1-Gal4 in the FeCO cell bodies. Magenta, RedStinger driven by each Gal4 line; Green, reference marker that labels all sensory neurons (ChAT-LexA; LexAop-nlsGFP).

Given that activation of AstA and Ms releasing neurons induces robust changes to locomotion (stopping or high-speed locomotion), we hypothesized that these neuropeptides may modulate sensory neurons in the leg in a state-dependent manner. To this end, we chose to focus specifically on AstAR1 and MsR1 expression in the leg sensory neurons. Looking closely at the expression of AstAR1 and MsR1 in the sensory axons of the T1 neuropils, we observe hallmark expression of AstAR1 and MsR1 in the femoral chordotonal organ (FeCO), as depicted by iav-Gal4>UAS-GFP (**Figure 3.2A**). Additionally, we observed expression of AstAR1 in bristle axons. The FeCO is the largest somatosensory structure in the fly leg and senses movement and kinematics of the femur-tibia joint[34,35]. The expression of AstAR1 and MsR1 in this important somatosensory structure suggests that AstA and Ms could flexibly modulate sensory thresholds in certain contexts. For example, AstA could be released broadly during rest and suppress FeCO activity to reduce transmission of leg movement sensory activity. In contrast, Ms could be released during high-speed locomotion and facilitate FeCO activity to optimize somatosensory feedback for movement. The FeCO is composed of at least 3 functionally and anatomically distinct subtypes: claw, club, and hook. Each subtype responds to different aspects of leg movement and sensation: position, movement, or vibration of the leg. AstA and Ms may modulate the FeCO broadly to generally suppress somatosensation, or it could target specific subtypes and thus, particular aspects of FeCO sensing. Thus, we looked at expression of AstAR1 and MsR1 in the cell bodies of the FeCO neurons in the leg to quantify which subtypes each neuropeptide targets. Here, we see broad expression of AstAR1-Gal4 and MsR1-Gal4 in the cell bodies of the FeCO (**Figure 3.2B)**. Specifically for AstAR1, we see expression in some but not all of the cells of the FeCO (**Figure 3.2C)**.

In conclusion, we observe expression of AstA and Ms receptors in FeCO sensory neurons, indicating a role for these neuropeptides in modulating somatosensory feedback onto motor circuits. Interestingly, we found differential receptor expression in the FeCO, indicating that AstA and Ms perform compartmentalized roles in modulating different aspects of FeCO sensing.

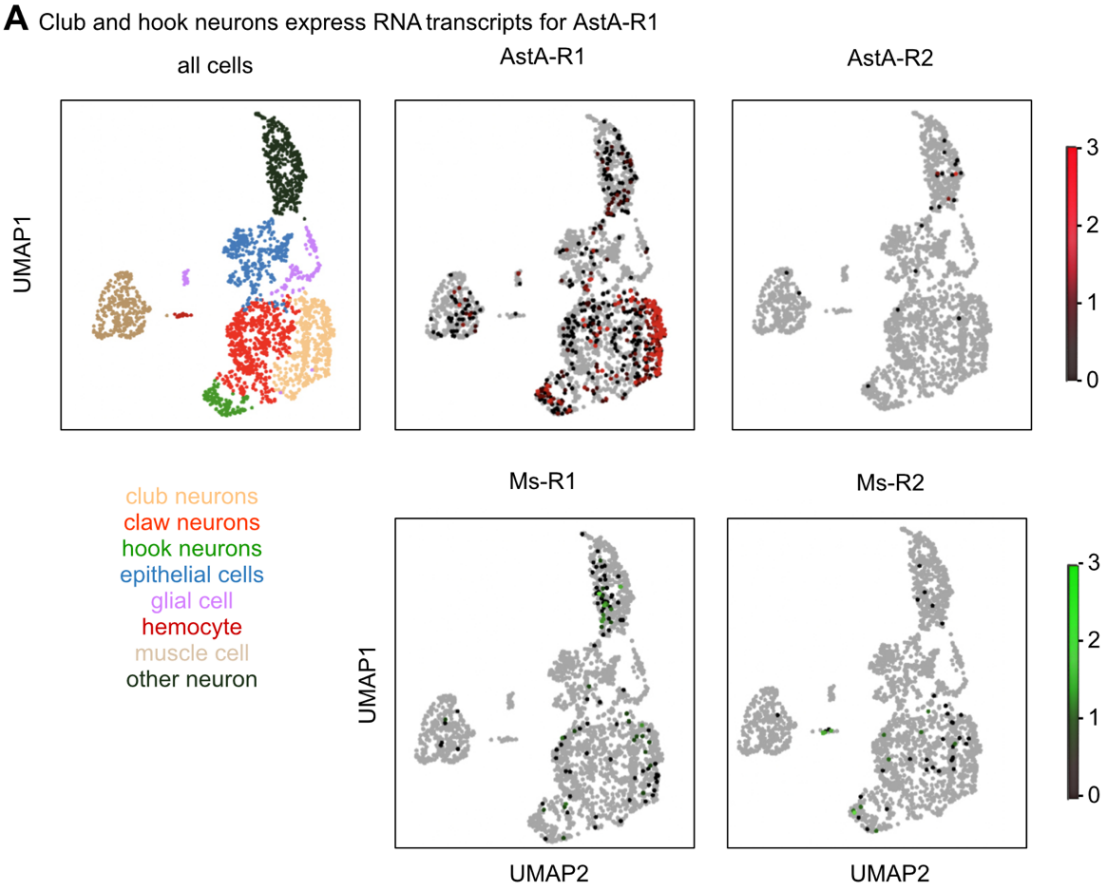

Figure 3.3 Expression of RNA transcripts in cells within the leg. (A) Uniform manifold approximation and projection (UMAP) visualization of annotated cell types within the leg. (B) AstAR1, AstAR2, MsR1, MsR2 expression levels with respect to annotated cell type clusters.

RNA-seq analysis of neuropeptide receptor expression in leg sensory neurons

We used genetic driver lines targeting AstAR1 and MsR1 to identify receptor expression in the FeCO sensory neurons. To further confirm if these receptors are expressed within FeCO sensory neurons, we analyzed the expression of AstA and Ms RNA transcripts in a single-nucleus

RNA-sequencing (RNA-seq) dataset of FeCO neurons in the Drosophila leg **(Figure 3.3A)**[35]. Using this additional method, we confirm that AstAR1 transcripts and not AstAR2 transcripts are expressed in the FeCO cell bodies. Specifically, we see that AstAR1 is expressed in the club and hook subtypes of the FeCO, suggesting selective modulation of particular aspects of FeCO sensing. Surprisingly, we see little to no expression of Ms receptors in the FeCO neurons (**Figure 3.3A)**. Although this stands in contrast to the anatomical expression of the genetic driver line, this does not rule out the possibility that Ms receptors are expressed in FeCO neurons. Since the RNA-seq data is collected exclusively from cell bodies in the leg, perhaps the Ms receptors are primarily located on the axons in the VNC.

AstA and Ms modulation of vibration sensing in the fly leg

Altogether, we find that AstAR1 is selectively expressed in the club and hook subtypes of the FeCO. Club neurons are sensitive to vibration of the leg and hook neurons are tuned to phasic movement of the femur-tibia joint. AstAR1 is a GIRK1 channel[46], indicating that AstA has an inhibitory effect on subpopulations of FeCO activity. MsR1 is a Gαi receptor[47,48] , which has a suppressive effect on muscle and cardiac activity in insects and crustaceans[49–52]. Similar to AstA, we predict that Ms has an inhibitory effect on FeCO activity. Considering the expression of AstA and Ms receptors in the FeCO neurons, we next tested the modulatory effects of the peptides on vibration sensitivity.

We recorded calcium responses from FeCO axons in the VNC while applying a range of vibration stimulus frequencies to the tibia of the fly and bath applying AstA or Ms peptide (**Figure 3.4A, B**). We observed no significant changes to activity in control or drug conditions across the range of frequencies (**Figure 3.4C, D**). Although these results are inconclusive, it does not exclude

the possibility that AstA and Ms modulate FeCO neurons in the fly as there could be other untested concentrations and contexts that drive a modulatory effect.

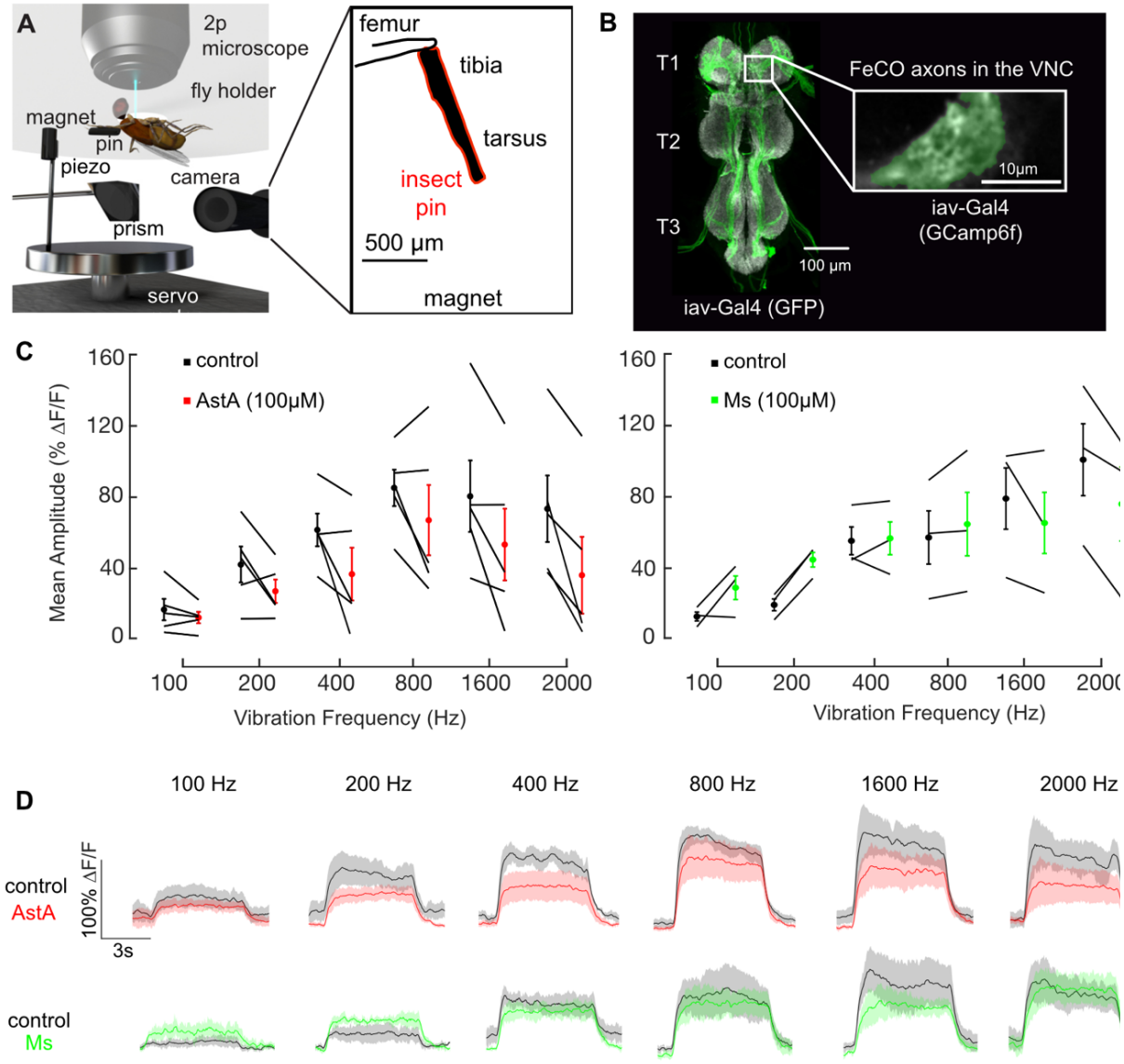

Figure 3.4 Bath application of AstA and Ms peptides. (A) Experimental set-up to record calcium activity from FeCO axons in the VNC with 2-photon microscopy while applying a 4s vibration stimulus to the fly's tibia and perfusing saline or peptide solutions. (B) Schematic depicting the imaging ROI: medial portion of the FeCO axons (iav-Gal4>UAS-GCamp6f) in the front, left neuropil. (C) Mean amplitude change in fluorescence ± SEM across flies, plotted versus vibration stimulus. Lines show individual responses to vibration stimuli, averaged across repeat trials, in control and drug conditions. n.s. for all comparisons, Wilcoxon rank-sum. Left, bath application of AstA peptide (red), n = 5. Right, bath application of Ms peptide (green), n = 3. (D) Average ΔF/F traces in the club axons in the VNC while applying a vibration stimulus to the tibia at different frequencies in saline (black) and peptide solution conditions. Top, responses after bath application of 100 uM AstA solution (red). Bottom, responses to bath application of 100 uM Ms solution (green). Lines depict mean responses ± SEM across flies.

3.4 Discussion

Neuromodulatory systems regulate locomotion behaviors in fruit flies

We found that optogenetically activating neuromodulatory populations in *Drosophila* promotes robust, stereotyped behaviors such as stopping movement and running. Here, we investigate the activity of two neuropeptides: AstA and Ms, which represent two of several positive outcomes of the behavior screen. Activation of AstA releasing neurons causes flies to stop movement while activation of Ms releasing neurons induces high-speed running (>30 mm/s). Although the genetic driver lines activate broad populations of neurons, it is surprising that the activation promotes a consistent and identifiable change in behavior. Even after introduction of Gal80 suppressors and altering the stimulating light intensity to restrict neural expression and recruitment, we still observed the robust changes to behavior. We hypothesized that AstA and Ms could promote a global state change, such as quiescence or high alertness which would necessitate the resulting changes in motor behavior.

Expression of AstA and Ms receptors in leg mechanosensory neurons

Using genetic driver lines and RNA-seq analysis, we characterized the expression of AstA and Ms neuromodulatory systems in central circuits and the leg. We find that neurons in the VNC release AstA and Ms, suggesting that these neuropeptides modulate sensorimotor circuits central to the VNC and periphery. Additionally, we find that AstA receptors (AstAR1 not AstAR2) are expressed in subtypes of the femoral chordotonal organ, a mechanosensory structure that senses proprioceptive and vibration information in the leg. The results for Ms receptor expression are less clear. While the genetic driver line for MsR1 reveals expression in the FeCO, this is not corroborated by RNA-seq analysis of FeCO neurons. This may be due to leaky expression in the

genetic driver line or the receptors could be expressed in the central axons and not the cell body in the periphery. In order to answer this question, we would need to use methods such as antibody staining to characterize the specific location of these receptors within the cell.

Overall, the selective expression of AstA and Ms receptors in leg sensory neurons raise questions on the functional relevance for modulation of primary sensory neurons and the relationship to the behavior observed. For example, there is evidence that AstA released to regulate sleep and hunger[53,54], while Ms activity is implicated in regulating enteroendocrine systems after mating[55]. In these particular states, it may be advantageous to strongly suppress sensory neuron activity to raise the threshold for arousal or behavioral response.

Pharmacology and calcium imaging to probe modulation of intact circuits

We applied pharmacology and calcium imaging methods to probe the modulatory effects of AstA and Ms on femoral chordotonal (FeCO) axons in the VNC. We found that exogenous application of AstA peptide had generally suppressive but not statistically significant effects on vibration sensing in FeCO neurons while application of Ms produced mixed responses. Prior work in the brain show that AstA is involved in regulating sleep-wake circuits in the brain and broad knockdown of AstA release promotes hyperarousal[21,22]. AstA could act diffusely across the nervous system to employ suppressive mechanisms, including suppressing mechanosensation to reduce thresholds for arousal.

Although our results were inconclusive, this does not exclude the possibility that AstA and Ms play a role in modulating FeCO sensing. There are a few caveats in this experiment: first, there are issues with the peptide concentration. In the experimental set-up, we are uncertain how much of the peptide solution reaches the neurons as the chemicals need to cross the glial sheath, then get

diluted in the hemolymph. Neuropeptides are known to have dose-dependent responses, so the effective concentration is relevant. Second, neuropeptides act in a context-dependent manner. We did not test a variety of states, for example by increasing arousal or inducing fictive locomotion, to better probe if there is a context-dependence to the effect of the neuropeptide.

Looking Forward

Altogether, we present experimental approaches to characterize neuromodulatory systems with a special emphasis on the ventral nerve cord and periphery. We delve into the modulatory role of AstA and Ms on sensorimotor circuits that control walking and vibration sensing of the FeCO. Ultimately, we hit a roadblock when trying to probe the functional context under which the modulation is used and endogenous sources of release. Critical to understanding the context-dependent modulation is having a foundational understanding of how FeCO information is used and the supporting neural circuitry. Therefore we chose to move on to other projects investigating the anatomy, circuitry, and function of FeCO neurons, as outlined in Chapter 1.

3.5 Acknowledgments

We thank members of the Tuthill laboratory for technical assistance and feedback on this project and manuscript. We thank Anne Sustar, Yanyan Qi, Tzu-Chiao Lu, and Hongjie Li for providing the single cell RNA-seq dataset of FeCO neurons for our analysis. We thank Matthew Banghart for assistance in custom synthesis of peptides for bath application. This work was supported by a Sloan Research Fellowship, the New York Stem Cell Foundation, and NIH grants R01NS102333 and U19NS104655 to J.C.T., and NIH grant T32 NS 99578-3 to S.J.L. and J.C.T.

3.6 Methods

Experimental Animals

Drosophila melanogaster were raised on standard cornmeal molasses food and housed in an incubator kept at 25°C on a 14:10 light dark cycle.

Optogenetic activation behavior experiments and analysis

To drive expression of Chrimson, we housed adult flies in cornmeal-molasses food with dissolved all-trans-retinal (35 mM in 95% EtOH, Santa Cruz Biotechnology) and in the dark for at least 24 hr before experiments. We tested groups of 2-5 day old flies, separated by sex, in a 10 cm circular arena fitted with a glass top. The arena is illuminated from below by infrared LEDs. For optogenetic activation, a red LED (625 nm-peak wavelength; ThorLabs) illuminated the arena from the top. Fly behaviors were recorded with a top-down view camera at 33 Hz (Basler acA1300-200 μm; Basler AG) mounted with a lens (Computar). Videos were tracked and analyzed using Ctrax software and MATLAB packages (Branson et al. 2009) and custom MATLAB scripts.

Sample preparation for confocal imaging of brains, VNCs, and legs

For confocal imaging of AstA, AstAR1, AstAR2, and MsR1 expressing neurons in the brain and VNC, we followed a protocol to dissect, stain, and mount the tissues. For preparation of brains and VNCs, we crossed flies carrying the GAL4 driver to flies carrying pJFRC7-20XUAS-IVS-mCD8::GFP. Using fine forceps, we dissected the brain and VNC out of adult flies in PBS or fly saline. Immediately after dissection, we fixed the tissue in 4% paraformaldehyde PBS solution for 15 min.After fixation, we rinsed in PBS three times then replaced the PBS with blocking solution (5% normal goat serum in PBS with 0.2% Triton-X) and incubated for 20 min. Next, we stained

the tissue in primary antibody solution (chicken anti-GFP antibody 1:50; anti-brp mouse for nc82 neuropil staining 1:50 in blocking solution) for 24 hr at room temperature. After primary incubation, we washed the tissue three times in PBST (PBS with 0.2% Triton-X), then incubated the tissue in secondary antibody solution (anti-chicken Alexa 488 1:250; anti-mouse Alexa 633 1:250 in blocking solution) for 24 hr at room temperature. After secondary incubation, we washed the tissue in PBST three times then mounted the tissue onto a slide with Vectashield (Vector Laboratories). We used a confocal microscope (Zeiss 510) to acquire z-stack images.

For confocal imaging of AstAR1 and MsR1 expressing neurons in the sensory neurons in the leg, we crossed flies carrying the GAL4 driver to flies carrying pJFRC7-20XUAS-IVS- mCD8::GFP. For co-labelling with cholinergic sensory neurons, we crossed flies carrying the GAL4 driver to flies carrying UAS-RedStinger; LexAopnlsGFP/CyO; ChAT-LexA/TM6B. We dissected legs while flies were anesthetized with CO_2. After dissection, the legs were fixed in 4% formaldehyde in PBS with 0.2% Triton-X for 20 minutes, then rinsed in PBS three times. The legs were mounted on a slide with Vectashield (Vector Laboratories). We used a confocal microscope (Zeiss 510) to acquire z-stack images.

Single-cell RNA-seq analysis

The methods for collection of the dataset and RNA-seq analysis are outlined as in Mamiya et al (2023). We accessed the dataset using SCope, an online platform for hosting and analyzing RNA-seq datasets.

Fly dissection for calcium imaging

We crossed flies carrying the GAL4 driver to flies carrying the GCamp6f calcium indicator and the structural marker tdTomato for reference. We followed the fly dissection protocol described in Mamiya et al (2018). Briefly, we mounted the flies into a custom holder with the head and thorax exposed on the top for imaging access and the legs and abdomen on the bottom for stimulus application. We glued down the legs and abdomen to restrict movement and interference with stimulus application to the front, right leg. We glued down the femur of the front, right leg and attached an insect pin to the tibia and tarsus. Next, we filled the recording chamber with fly saline and removed the cuticle covering the prothoracic neuropil of the VNC. Lastly, we pierced the glial sheath using sharpened, fine forceps to promote diffusion across the blood-brain barrier.

In vivo two-photon image acquisition

We used a two-photon Movable Objective Microscopes (MOM; Sutter Instruments) with a 20x water-immersion objective (Olympus XLUMPlanFI, 0.95 NA, 2.0 mm wd; Olympus) and a 40x water-immersion objective (0.8 NA, 2.0 mm wd; Nikon Instruments) for imaging. We used a mode-locked Ti:sapphire laser (Chameleon Vision S; Coherent) to excite fluorophores at 920 nm. We maintained power at the back aperture of the objective below ~35 mW with a Pockels cell. Emitted fluorescence was directed to two high-sensitivity GaAsP photomultiplier tubes (Hamamatsu Photonics) through a 705 nm edge dichroic beamsplitter followed by a 580 nm edge image splitting dichroic beamsplitter (Semrock). Fluorescence was band-passed filtered by either a 525/50 (green) or 641/75 (red) emission filter (Semrock). Image acquisition was controlled with ScanImage 5.2 (Vidrio Technologies) in MATLAB (MathWorks). Each microscope was equipped with a galvo-resonant scanner, and each objective was mounted onto a piezo actuator (Physik Instrumente; digital piezo controller E-709). We focused our recordings on the medial region of

the front, left neuropil, which contains the greatest region of vibration-sensitive axons (Mamiya et al. 2018). All experiments were performed in the dark at room temperature.

AstA and Ms Peptides

AstA (SRPYSFGL-NH2) and Ms (TDVDHVFLRF-NH2) peptides were synthesized and acquired from Biomatik. Peptide solutions were stored in 1mM stock solutions and diluted in saline to experimental concentrations.

During experiments, fly saline was constantly perfused over the fly's VNC. For peptide bath application experiments 100 uM AstA or Ms solution (AstA and Ms peptide; Biomatik dissolved in saline) was perfused onto the preparation. Perfusion lines were washed with 70% EtOH in DI water, then fresh saline before starting a new preparation.

Vibrating the tibia with a piezoelectric crystal system

We used a magnet-piezoelectric system (PA3JEW, Max displacement 1.8 μm; ThorLabs) described in detail in Mamiya et al 2018 to apply a vibration stimulus to the tibia of the fly's leg. We used custom MATLAB scripts to generate 100-2000Hz vibration frequency stimuli. The stimuli were delivered through a single channel open-loop piezo controller (ThorLabs). Each vibration stimulus was presented for 4s, two times, with an inter-stimulus interval of 8s.

Calcium imaging analysis

Calcium imaging data was analyzed using custom MATLAB scripts. We applied K-means to identify vibration-sensitive pixels in the ROI. We compared activity in the same regions before

and after bath application of the synthesized peptides. We calculated the mean amplitude change in fluorescence after vibration the tibia by calculating the difference between the mean response during the 4s stimulus period and a 4s baseline period preceding the stimulus.

References

1. Sombati, S. & Hoyle, G. Generation of specific behaviors in a locust by local release into neuropil of the natural neuromodulator octopamine. *J. Neurobiol.* **15**, 481–506 (1984).
2. Orchard, I., Ramirez, J. M. & Lange, A. B. A Multifunctional Role for Octopamine in Locust Flight. *Annu. Rev. Entomol.* **38**, 227–249 (1993).
3. Ramirez, J. M. & Pearson, K. G. Octopaminergic modulation of interneurons in the flight system of the locust. *J. Neurophysiol.* **66**, 1522–1537 (1991).
4. Suver, M. P., Mamiya, A. & Dickinson, M. H. Octopamine Neurons Mediate Flight-Induced Modulation of Visual Processing in *Drosophila*. *Curr. Biol.* **22**, 2294–2302 (2012).
5. Tuthill, J. C., Nern, A., Rubin, G. M. & Reiser, M. B. Wide-field feedback neurons dynamically tune early visual processing. *Neuron* **82**, 887–895 (2014).
6. Bodily changes in pain, hunger, fear and rage: an account of recent researches into the function of emotional excitement - Digital Collections - National Library of Medicine. https://collections.nlm.nih.gov/catalog/nlm:nlmuid-00620620R-bk?_gl=1*kmchx0*_ga*MTM2NjE5MjM5OS4xNjg3MzgzNjE5*_ga_7147EPK006*MTcxMzIxODM2My4xLjEuMTcxMzIxODQ0NC4wLjAuMA..*_ga_P1FPTH9PL4*MTcxMzIxODM2My4xLjEuMTcxMzIxODQ0NC4wLjAuMA..
7. Bargmann, C. I. Beyond the connectome: How neuromodulators shape neural circuits. *BioEssays* **34**, 458–465 (2012).
8. Marder, E. Neuromodulation of Neuronal Circuits: Back to the Future. *Neuron* **76**, 1–11 (2012).

9. Miles, G. B. & Sillar, K. T. Neuromodulation of Vertebrate Locomotor Control Networks. *Physiology* **26**, 393–411 (2011).

10. Nadim, F. & Bucher, D. Neuromodulation of Neurons and Synapses. *Curr. Opin. Neurobiol.* **0**, 48–56 (2014).

11. Harris-Warrick, R. M. Neuromodulation and Flexibility in Central Pattern Generator Networks. *Curr. Opin. Neurobiol.* **21**, 685–692 (2011).

12. Marder, E. Neuromodulation of Neuronal Circuits: Back to the Future. *Neuron* **76**, 1–11 (2012).

13. Brand, A. H. & Perrimon, N. Targeted gene expression as a means of altering cell fates and generating dominant phenotypes. *Development* **118**, 401–415 (1993).

14. Fire, A. *et al.* Potent and specific genetic interference by double-stranded RNA in Caenorhabditis elegans. *Nature* **391**, 806–811 (1998).

15. Deng, B. *et al.* Chemoconnectomics: Mapping Chemical Transmission in Drosophila. *Neuron* **101**, 876-893.e4 (2019).

16. Tian, L. *et al.* Imaging neural activity in worms, flies and mice with improved GCaMP calcium indicators. *Nat. Methods* **6**, 875–881 (2009).

17. Hodge, J. J. L. Ion Channels to Inactivate Neurons in Drosophila. *Front. Mol. Neurosci.* **2**, 13 (2009).

18. Bernstein, J. G., Garrity, P. A. & Boyden, E. S. Optogenetics and thermogenetics: technologies for controlling the activity of targeted cells within intact neural circuits. *Curr. Opin. Neurobiol.* **22**, 61–71 (2012).

19. Donlea, J. M. Neuronal and molecular mechanisms of sleep homeostasis. *Curr. Opin. Insect Sci.* **24**, 51–57 (2017).

20. Hulse, B. K. *et al.* A connectome of the Drosophila central complex reveals network motifs suitable for flexible navigation and context-dependent action selection. *eLife* **10**, e66039.

21. Donlea, J. M. *et al.* Recurrent Circuitry for Balancing Sleep Need and Sleep. *Neuron* **97**, 378-389.e4 (2018).

22. Ni, J. D. *et al.* Differential regulation of the Drosophila sleep homeostat by circadian and arousal inputs. *eLife* **8**, e40487 (2019).

23. Donlea, J. M., Thimgan, M. S., Suzuki, Y., Gottschalk, L. & Shaw, P. J. Inducing Sleep by Remote Control Facilitates Memory Consolidation in Drosophila. *Science* **332**, 1571–1576 (2011).

24. Shafer, O. T. & Keene, A. C. The Regulation of *Drosophila* Sleep. *Curr. Biol.* **31**, R38–R49 (2021).

25. Stoleru, D., Peng, Y., Agosto, J. & Rosbash, M. Coupled oscillators control morning and evening locomotor behaviour of Drosophila. *Nature* **431**, 862–868 (2004).

26. Artiushin, G. & Sehgal, A. The *Drosophila* circuitry of sleep–wake regulation. *Curr. Opin. Neurobiol.* **44**, 243–250 (2017).

27. Grima, B., Chélot, E., Xia, R. & Rouyer, F. Morning and evening peaks of activity rely on different clock neurons of the Drosophila brain. *Nature* **431**, 869–873 (2004).

28. Pfeiffenberger, C., Lear, B. C., Keegan, K. P. & Allada, R. Locomotor activity level monitoring using the Drosophila Activity Monitoring (DAM) System. *Cold Spring Harb. Protoc.* **2010**, pdb.prot5518 (2010).

29. Faville, R., Kottler, B., Goodhill, G. J., Shaw, P. J. & van Swinderen, B. How deeply does your mutant sleep? Probing arousal to better understand sleep defects in Drosophila. *Sci. Rep.* **5**, 8454 (2015).

30. Liu, S., Liu, Q., Tabuchi, M. & Wu, M. N. Sleep Drive Is Encoded by Neural Plastic Changes in a Dedicated Circuit. *Cell* **165**, 1347–1360 (2016).

31. Pimentel, D. *et al.* Operation of a Homeostatic Sleep Switch. *Nature* **536**, 333–337 (2016).

32. Dissel, S. *et al.* Sleep-promoting neurons remodel their response properties to calibrate sleep drive with environmental demands. *PLOS Biol.* **20**, e3001797 (2022).

33. Jones, J. D. *et al.* Regulation of sleep by cholinergic neurons located outside the central brain in Drosophila. *PLoS Biol.* **21**, e3002012 (2023).

34. Mamiya, A., Gurung, P. & Tuthill, J. C. Neural Coding of Leg Proprioception in Drosophila. *Neuron* **100**, 636-650.e6 (2018).

35. Mamiya, A. *et al.* Biomechanical origins of proprioceptor feature selectivity and topographic maps in the *Drosophila* leg. *Neuron* **111**, 3230-3243.e14 (2023).

36. Zill, S. N. Selective mechanical stimulation of an identified proprioceptor in freely moving locusts: role of resistance reflexes in active posture. *Brain Res.* **417**, 195–198 (1987).

37. Usherwood, P. N. R., Runion, H. I. & Campbell, J. I. Structure and Physiology of A Chordotonal Organ in the Locust Leg. *J. Exp. Biol.* **48**, 305–323 (1968).

38. Mendes, C. S., Bartos, I., Akay, T., Márka, S. & Mann, R. S. Quantification of gait parameters in freely walking wild type and sensory deprived Drosophila melanogaster. *eLife* **2**, (2013).

39. McKelvey, E. G. Z. *et al.* Drosophila females receive male substrate-borne signals through specific leg neurons during courtship. *Curr. Biol. CB* **31**, 3894-3904.e5 (2021).

40. Nusbaum, M. P. & Blitz, D. M. Neuropeptide modulation of microcircuits. *Curr. Opin. Neurobiol.* **22**, 592–601 (2012).

41. Lundberg, J. M. & Hökfelt, T. Coexistence of peptides and classical neurotransmitters. *Trends Neurosci.* **6**, 325–333 (1983).

42. Arrigoni, E. & Saper, C. B. What optogenetic stimulation is telling us (and failing to tell us) about fast neurotransmitters and neuromodulators in brain circuits for wake-sleep regulation. *Curr. Opin. Neurobiol.* **0**, 165–171 (2014).

43. Muschol, M. & Salzberg, B. M. Dependence of Transient and Residual Calcium Dynamics on Action-Potential Patterning during Neuropeptide Secretion. *J. Neurosci.* **20**, 6773–6780 (2000).

44. Li, L. *et al.* Activity-dependent constraints on catecholamine signaling. *Cell Rep.* **42**, 113566 (2023).

45. Nässel, D. R. Substrates for Neuronal Cotransmission With Neuropeptides and Small Molecule Neurotransmitters in Drosophila. *Front. Cell. Neurosci.* **12**, (2018).

46. Birgül, N., Weise, C., Kreienkamp, H. J. & Richter, D. Reverse physiology in drosophila: identification of a novel allatostatin-like neuropeptide and its cognate receptor structurally related to the mammalian somatostatin/galanin/opioid receptor family. *EMBO J.* **18**, 5892–5900 (1999).

47. Egerod, K. *et al.* Molecular cloning and functional expression of the first two specific insect myosuppressin receptors. *Proc. Natl. Acad. Sci.* **100**, 9808–9813 (2003).

48. Johnson, E. C. *et al.* Identification of *Drosophila* Neuropeptide Receptors by G Protein-coupled Receptors-β-Arrestin2 Interactions*. *J. Biol. Chem.* **278**, 52172–52178 (2003).

49. Lange, A. B., Orchard, I. & Te Brugge, V. A. Evidence for the involvement of a SchistoFLRF-amide-like peptide in the neural control of locust oviduct. *J. Comp. Physiol. A* **168**, 383–391 (1991).

50. Zhou, Y. J., Seike, H. & Nagata, S. Function of myosuppressin in regulating digestive function in the two-spotted cricket, *Gryllus bimaculatus*. *Gen. Comp. Endocrinol.* **280**, 185–191 (2019).

51. Holman, G. M., Cook, B. J. & Nachman, R. J. Primary structure and synthesis of a blocked myotropic neuropeptide isolated from the cockroach, *Leucophaea maderae*. *Comp. Biochem. Physiol. Part C Comp. Pharmacol.* **85**, 219–224 (1986).

52. Stevens, J. S. *et al.* The peptide hormone pQDLDHVFLRFamide (crustacean myosuppressin) modulates the Homarus americanus cardiac neuromuscular system at multiple sites. *J. Exp. Biol.* **212**, 3961–3976 (2009).

53. Chen, J. *et al.* Allatostatin A Signalling in Drosophila Regulates Feeding and Sleep and Is Modulated by PDF. *PLOS Genet.* **12**, e1006346 (2016).

54. Hergarden, A. C., Tayler, T. D. & Anderson, D. J. Allatostatin-A neurons inhibit feeding behavior in adult Drosophila. *Proc. Natl. Acad. Sci. U. S. A.* **109**, 3967–3972 (2012).

55. Hadjieconomou, D. *et al.* Enteric neurons increase maternal food intake during reproduction. *Nature* **587**, 455–459 (2020).

Chapter 4

FUTURE DIRECTIONS

In this thesis, we investigate the circuit and neuromodulation of the femoral chordotonal organ (FeCO) in *Drosophila* to discern its ethological functions. In Chapter 2, we constructed the first connectome of the largest somatosensory structure in the fruit fly leg, comprehensively mapping the feedback pathways from the FeCO onto local and global motor programs. This work bolsters our understanding of the FeCO's role as an important proprioceptor for local leg control and also generates new, testable hypotheses about its function. Unexpectedly, we found that vibration-sensitive FeCO neurons synapse onto divergent circuits from the proprioceptive pathway and integrate with auditory circuits in the brain. This finding provides evidence for the emerging hypothesis that the *Drosophila* FeCO functions as an exteroceptor tuned to substrate vibrations. In Chapter 3, we investigate state-dependent neuromodulation of sensorimotor circuits and the FeCO, generating further hypotheses about how FeCO information is centrally transformed and modulated in functional contexts. In this Chapter, we will discuss future directions to test some of the predictions from Chapters 2 and 3.

Vibration sensing in *Drosophila*

The *Drosophila* FeCO is typically described as a proprioceptive structure that detects position and movement of the leg[3–5]. In addition to its proprioceptive capacities however, the FeCO

also senses vibration, further complicating its study[6]. In fact, a significant number of FeCO neurons are vibration sensitive: in the front, left leg 66 out of 152 of the neurons respond to leg vibration[7]. Little is known about the ethological relevance of substrate vibration information in *Drosophila*, so it is unclear if the FeCO detects functionally relevant vibration signals or if this is a by-product of its sensitivity to bidirectional movement. This is not a unique challenge to the *Drosophila* FeCO. In insects, all auditory structures tuned to external vibrations evolved from chordotonal organs but not all chordotonal organs are used for audition, even if responsive to vibration[1,2].

A logical next step from this work is to experimentally test if leg vibration sensors are serving an auditory purpose. First, it is important to probe the full range of vibration frequencies the animal is tuned to and the behavioral responses. Previous studies that record responses from FeCO neurons and downstream interneurons applied pure tone frequency stimuli to the leg (100Hz - 2000Hz)[6–9]. While these recordings show that the FeCO is responsive to vibration, it does not rigorously test the full spectrum of responses, especially to naturalistic stimuli. To accomplish this, it is feasible to record from FeCO axons and downstream interneurons while presenting a greater range of frequency stimuli as well as complex, naturalistic stimuli such as courtship song, movements from presumed predators, or environmental noises such as wind.

Startle/Escape Behaviors

Vibration-sensitive club neurons are indirectly connected to freezing and take-off flight motor programs: the long tendon muscle (LTM) and the peripherally synapsing interneuron (PSI)[10,11]. In Chapter 2, we proposed that the connectivity to startle and escape circuits suggests that the club neurons are wired for detecting externally-generated vibrations. Club neurons weakly converge onto the LTM and PSI through different sets of interneurons, suggesting context-

dependent activation of each respective motor neuron. Based on the connectivity between club neurons and motor neurons, we predict that a low amplitude brief stimulus may activate the LTM to induce freezing while a high amplitude, prolonged stimulus is necessary to activate the PSI for take-off. Additionally, input from vibration sensors alone may be sufficient to produce freezing, while multiple aversive sensory signals may be required to activate the energetically costly take-off behavior. Identifying the stimulus features that drive startle or escape responses will also aid in determining the ethologically relevant stimuli that vibration sensors are tuned to.

Courtship

Club neurons synapse onto multiple parallel, ascending pathways that integrate with auditory circuits in the brain. In Chapter 2, we mapped the pathways for integration of tactile vibrations from the leg and airborne vibrations from the antennae and proposed that these circuits are relevant for processing courtship-related sensory information. Male flies produce an airborne courtship song with their wings, which is actively modulated depending on how the female moves[12]. One underexplored aspect of courtship behavior is how airborne and substrate borne vibration information is used. In addition to "singing", recent evidence suggests that male flies also tap their abdomens on the substrate during courtship and females rely on FeCO sensing to detect this information[13,14]. In addition to tapping, there could be other salient substrate vibrations produced by movement of the courting animals or "noisy" substrate vibrations in the environment that need to be filtered out. In *Drosophila montana*, flies are less likely to engage in courtship when environmental acoustic noise interferes with their courtship signals[15]. Perhaps the leg vibration sensors are used to optimize sound localization, especially in noisy environments. To test the limits of hearing and spatial localization, we can quantify the success of courtship

environments in more naturalistic contexts, adding mechanical vibration distractors to probe the limits of vibration sensing while serially knocking down antennal and/or leg chordotonal organs.

Comparison of vibration sensing across the body

In Chapter 2, we introduce the first connectome of a leg mechanosensory structure in a limbed animal. In this work, we compared the proprioceptive and vibration sensing pathways within the FeCO circuit, but it will be interesting to further compare how processing of leg vibration information compares to other sensory systems, especially auditory circuits from the antennae. For example, leg vibration information is pooled across six legs and that information is through recurrently connected interneurons. This circuit architecture may be used for spatial localization, thus the information across the sensors needs to be compared with each other. Additionally, the legs can move both independently and in synchrony with each other, producing variable amounts of noise in the vibration signal that needs to be reduced. How does the circuit architecture for central processing of leg vibration compare to vibration information coming from two antennae, for example? In fruit flies, the Johnston's Organ in the antennae contains ~500 neurons[16]. Assuming the number of FeCO neurons are similar across legs, we predict there are ~900 neurons in total (this includes both proprioceptive and vibration sensing neurons). What are the outcomes for central processing of vibration information if you have sensors placed on spatially distributed and highly mobile tissues? Further, how does central processing of leg vibration compare to other modalities, such as tactile sensing from leg bristles? There are multiple, ongoing projects investigating the connectomes of other sensory modalities that project to the central nervous system, including wing mechanosensors, tactile leg bristles, and nociceptors on the abdomen. As we move towards a complete connectome of the entire fly central nervous system, I

am excited to see further comparisons of how somatosensation is processed and topographically represented – forming a somatosensory "homunculus" in the fly.

Context-dependent modulation of vibration sensing

While the FeCO proprioceptors are primarily involved in local, reflexive loops for leg motor control, the vibration sensors feed into multi-layer, long-range pathways that integrate the sensory signal across legs and to the brain. This circuit architectures presents many opportunities for investigating state-dependent modulation. Here, I will address a few topics to explore further.

Compartmentalized computation

From the FeCO connectome, we see that the leg vibration signal is pooled across the legs and projects to the brain. While we found evidence that frequency tuning of sensory neurons is conserved in the downstream circuitry, the highly recurrent circuit architecture also suggests that complex features can be processed and parsed within the VNC. Interneurons downstream of the vibration sensors have projections in all six legs and project to the brain. We found evidence of lateral inhibition and disinhibitory circuits that could tune the sensory signal within a leg and across legs. As stated earlier, recordings from FeCO neurons and downstream circuits are made in response to application of pure tone vibration frequencies applied to the leg. How would the presentation of complex and ethologically relevant stimuli, such as courtship song or recordings of predator movements, affect the central processing? We predict that there will be different topographic organization in different compartments: 1) the primary sensory layer, 2) downstream neurons within a leg, and 3) ascending projections to the brain, as it seems likely that each compartment is tuned for contextually different information.

Neuromodulatory influence on FeCO sensing

Lastly, construction of the synaptic wiring diagram of the FeCO circuit was made possible due to the application of automated synapse detection methods to the EM dataset[11,17]. When considering state-dependent modulation, we also have to consider the role of neuromodulators that can act outside of the synapse. In Chapter 3, we found evidence that the neuropeptides, Allatostatin A and Myosuppressin, can modulate the FeCO. Dense core vesicles are visible within the EM dataset but we do not quite have the capacity to automatically detect dense core vesicles, but efforts are ongoing. As we move towards a more complete synaptic wiring diagram of the VNC, hopefully this can serve as a foundation to investigate the role of neuromodulation, similar to work done in *C. elegans* nervous systems and the stomatogastric ganglion of crustaceans[18–20].

References

1. Yack, J. E. & Fullard, J. H. What is an Insect Ear? *Ann. Entomol. Soc. Am.* **86**, 677–682 (1993).
2. Göpfert, M. C. & Hennig, R. M. Hearing in Insects. *Annu. Rev. Entomol.* **61**, 257–276 (2016).
3. Field, L. H. & Pflüger, H.-J. The femoral chordotonal organ: A bifunctional orthopteran (Locusta migratoria) sense organ? *Comp. Biochem. Physiol. A Physiol.* **93**, 729–743 (1989).
4. Zill, S. N. Selective mechanical stimulation of an identified proprioceptor in freely moving locusts: role of resistance reflexes in active posture. *Brain Res.* **417**, 195–198 (1987).
5. Mendes, C. S., Bartos, I., Akay, T., Márka, S. & Mann, R. S. Quantification of gait parameters in freely walking wild type and sensory deprived Drosophila melanogaster. *eLife* **2**, e00231 (2013).
6. Mamiya, A., Gurung, P. & Tuthill, J. C. Neural Coding of Leg Proprioception in Drosophila. *Neuron* **100**, 636-650.e6 (2018).
7. Mamiya, A. *et al.* Biomechanical origins of proprioceptor feature selectivity and topographic maps in the *Drosophila* leg. *Neuron* **111**, 3230-3243.e14 (2023).
8. Agrawal, S. *et al.* Central processing of leg proprioception in *Drosophila*. *eLife* **9**, e60299 (2020).
9. Chen, C. *et al.* Functional architecture of neural circuits for leg proprioception in *Drosophila*. *Curr. Biol.* **31**, 5163-5175.e7 (2021).
10. King, D. G. & Wyman, R. J. Anatomy of the giant fibre pathway in Drosophila. I. Three thoracic components of the pathway. *J. Neurocytol.* **9**, 753–770 (1980).

11. Azevedo, A. *et al.* Tools for comprehensive reconstruction and analysis of Drosophila motor circuits. 2022.12.15.520299 Preprint at https://doi.org/10.1101/2022.12.15.520299 (2022).

12. Coen, P. *et al.* Dynamic sensory cues shape song structure in Drosophila. *Nature* **507**, 233–237 (2014).

13. Fabre, C. C. G. *et al.* Substrate-Borne Vibratory Communication during Courtship in Drosophila melanogaster. *Curr. Biol.* **22**, 2180–2185 (2012).

14. McKelvey, E. G. Z. *et al.* Drosophila females receive male substrate-borne signals through specific leg neurons during courtship. *Curr. Biol.* **31**, 3894-3904.e5 (2021).

15. Samarra, F. I. P., Klappert, K., Brumm, H. & Miller, P. J. O. Background noise constrains communication: acoustic masking of courtship song in the fruit fly Drosophila montana. *Behaviour* **146**, 1635–1648 (2009).

16. Kamikouchi, A., Shimada, T. & Ito, K. Comprehensive classification of the auditory sensory projections in the brain of the fruit fly Drosophila melanogaster. *J. Comp. Neurol.* **499**, 317–356 (2006).

17. Buhmann, J. *et al.* Automatic detection of synaptic partners in a whole-brain Drosophila electron microscopy data set. *Nat. Methods* **18**, 771–774 (2021).

18. Ripoll-Sánchez, L. *et al.* The neuropeptidergic connectome of C. elegans. *Neuron* **111**, 3570-3589.e5 (2023).

19. Bargmann, C. I. Beyond the connectome: how neuromodulators shape neural circuits. *BioEssays News Rev. Mol. Cell. Dev. Biol.* **34**, 458–465 (2012).

20. Marder, E. Neuromodulation of Neuronal Circuits: Back to the Future. *Neuron* **76**, 1–11 (2012).